

5th Annual Workshop Prize-Winning Poster Abstracts

The "RAPID" High Rate Area X-ray Detector System

R.A. Lewis, C.Hall, B.Parker, A.Jones, W.Helsby, J.Sheldon, P.Clifford, M.Hillen. N.Fore.

CCLRC Daresbury Laboratory, Daresbury, Warrington, Cheshire WA4 4AD, U.K.

Abstract

Multiwire proportional counters (MWPCs) have been used for many years for small angle scattering and are particularly well suited to dynamic experiments. Their advantages include, almost zero noise, high dynamic range limited only by the electronic memory depth, large area and time frame resolutions of the order of tens of microseconds. They do, however, have some limitations, notably in global and local count rate performance.

The biological X-ray detector group at Daresbury has developed a two dimensional detector system which delivers a more than twenty-fold increase in throughput over the present systems. It comprises a "wire MicroGap" detector, which has much better local count rate performance than conventional MWPCs and a sophisticated multi-channel data acquisition system. The system has a global count rate capability of greater than 2×10^7 photons/sec with a maximum local count rate of greater than 10^6 photons/mm²/sec. A spatial resolution of $\sim 25\mu\text{m}$, over an active area of $12.8 \times 12.8\text{cm}^2$, has been achieved which compares well with existing readout systems. A $20 \times 20\text{cm}^2$ version is under development. Each electrode of the detector is instrumented with a preamplifier and ADC and the position of the event is determined independently in X and Y by centroiding the induced charge distribution. The X and Y co-ordinates are correlated using a unique time stamp. This paper describes the design and performance of the detector and readout system and presents some recent beamline results.

Introduction

The detectors which are currently used for small angle scattering are either count rate limited and therefore have to be attenuated (delay line MWPCs with a maximum rate of 10^6 photons/sec) or are noise

limited (image plates). A system capable of recording unattenuated diffraction patterns on the SRS with the same quality of data as is currently obtained with the delay line detectors opens up the possibility of higher time resolution experiments, less radiation damage or simply a considerable improvement in the overall throughput of work from the SRS.

RAPID, the **Refined ADC Per Input Detector** system is now undergoing preliminary beamline commissioning. It is a fast photon counting detector system with parameters similar to the existing delay line systems but with a factor of 20 improvement in count rate. The overall system specifications are given in Table 1.

RAPID System	
Detector type	Wire MicroGap
Active area of beamline detector	200mm x 200mm
Active area of prototype	128mm x 128mm
Maximum global counting rate	$> 10^6$ photons/sec/mm ²
Maximum local counting rate	$> 2 \times 10^7$ photons/sec
Upgradable to $\sim 10^8$ photons s ⁻¹	
Gas Filling	Xe Ar CO ₂
Drift depth	Adjustable, normally 15mm.
Efficiency @ 8 keV	80%
Number of pixels	Adjustable up to 8192 x 8192
Number of electronics channels	128x128 expandable to 256x256
Spatial Resolution	$\sim 250\mu\text{m}$ fwhm
Noise Level	$\sim 2.5 \times 10^{-4}$ cts/mm ² /s ¹
Number of frames	Variable depending on amount of memory. Up to 1024 images of 1024x1024 pixels or 4096 images of 512x512 pixels etc.
Time resolution	100ns
Spectral resolution	$\sim 20\%$ fwhm @ 8 keV

Table 1 Specifications of the RAPID data acquisition system

System description

RAPID consists of three parts.

1) A two dimensional wire MicroGap detector.

The new Daresbury-developed wire MicroGap detector technology yields a local count rate performance of approximately 10^6 photons/mm²/sec which is some two orders of magnitude greater than the conventional MWPC detectors. A wire MicroGap device is a central feature of the multiwire linear

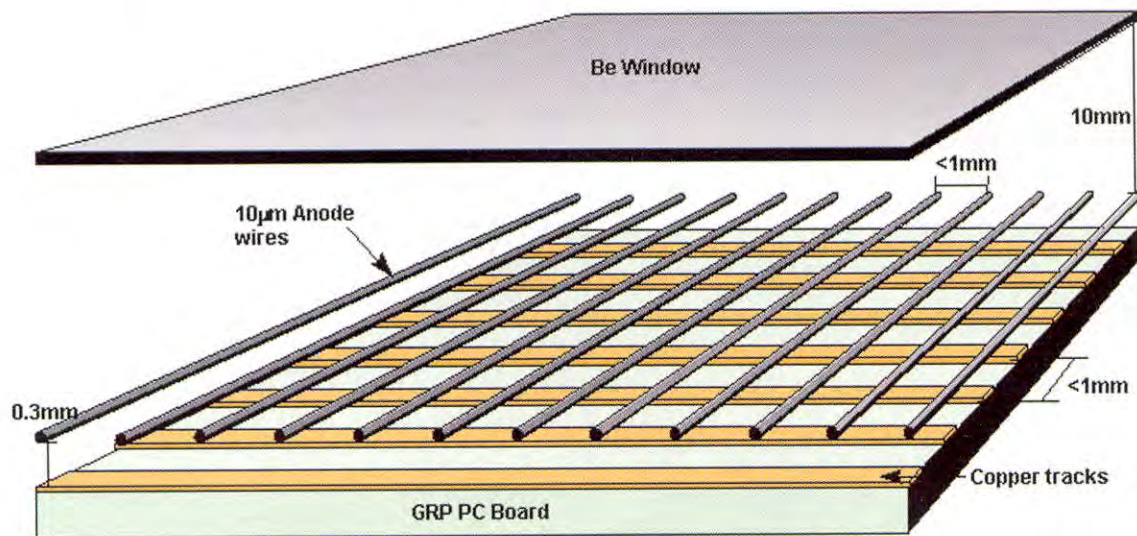


Figure 1 The two dimensional wire MicroGap detector

detector [1] which has been operational in various forms for five years [2]. The local count rate performance is such that it has proved capable of handling completely unattenuated diffraction patterns on station 16.1 which is the most intense X-ray source on the SRS.

The prototype RAPID detector is a two dimensional version of this technology with 128×128 electrodes on a 1mm pitch. The primary charge is spread over at least 2 anodes after it has drifted in from the point of interaction above the plane of the anode wires. With two or more anodes sharing the primary charge, interpolation can be performed on both anodes and cathodes; the signals for one co-ordinate are taken from the anode, whilst the others are taken from the cathode. The signal distribution on the anode channels is predictably quite different to that on the cathodes but this can be readily accommodated by the data acquisition system. In order to increase the active area, another detector having an active area of $200 \times 200 \text{mm}^2$ but maintaining the 128×128 readout channels is under construction. The spatial resolution will be maintained by the use of a charge sharing network connecting the electrodes.

2) A very fast multi-channel data acquisition system

Due to the extreme complexity of the system, only a brief description follows. What follows is a short description of its operation. Each anode wire and cathode strip from the chamber is connected to one channel of the readout system. The signal path is split into two, one is with a 40ns shaping time connected to the 8 bit flash ADC, whilst the other has a faster 10ns shaping time and is connected to a

discriminator. The discriminator thresholds and amplifier gains and offsets are all individually adjustable from the software.

The ADCs normally free run at 80Mhz but when an event occurs, the discriminator outputs are used to adjust the clocks of the ADCs most closely surrounding the event. This then ensures that the pulse is sampled at its peak. The previous samples taken during free running mode are then subtracted from the peak samples to provide pulse height measurements with high immunity from pulse pile-up. Four neighbouring ADC channels in each dimension are simultaneously coincidentally triggered on each event. The pulse height data and a time stamp taken from the $\sim 160 \text{Mhz}$ master clock are communicated across a back-plane bus to the controller. Three of the four pulse height data are then selected to make the fine position and pulse height measurements which are performed. This is achieved using look up RAMs which contain data pre-calculated from the position and height algorithms. The coarse position of the event is derived from the pattern of discriminator hits.

The separate X and Y co-ordinates, which are derived from a combination of the fine and coarse positions, are time tagged to an accuracy of $\sim 6.25 \text{ns}$ and these data are then stored in dual ported RAMs for use by the X-Y correlator. This unit checks the temporal validity of the separate data, puts the X and Y data together with some error grading information on a bus and then transfers the data which then latched into the DL200 histogramming memory. Each electrode of the detector is instrumented with a preamplifier and ADC. The ADC samples from the

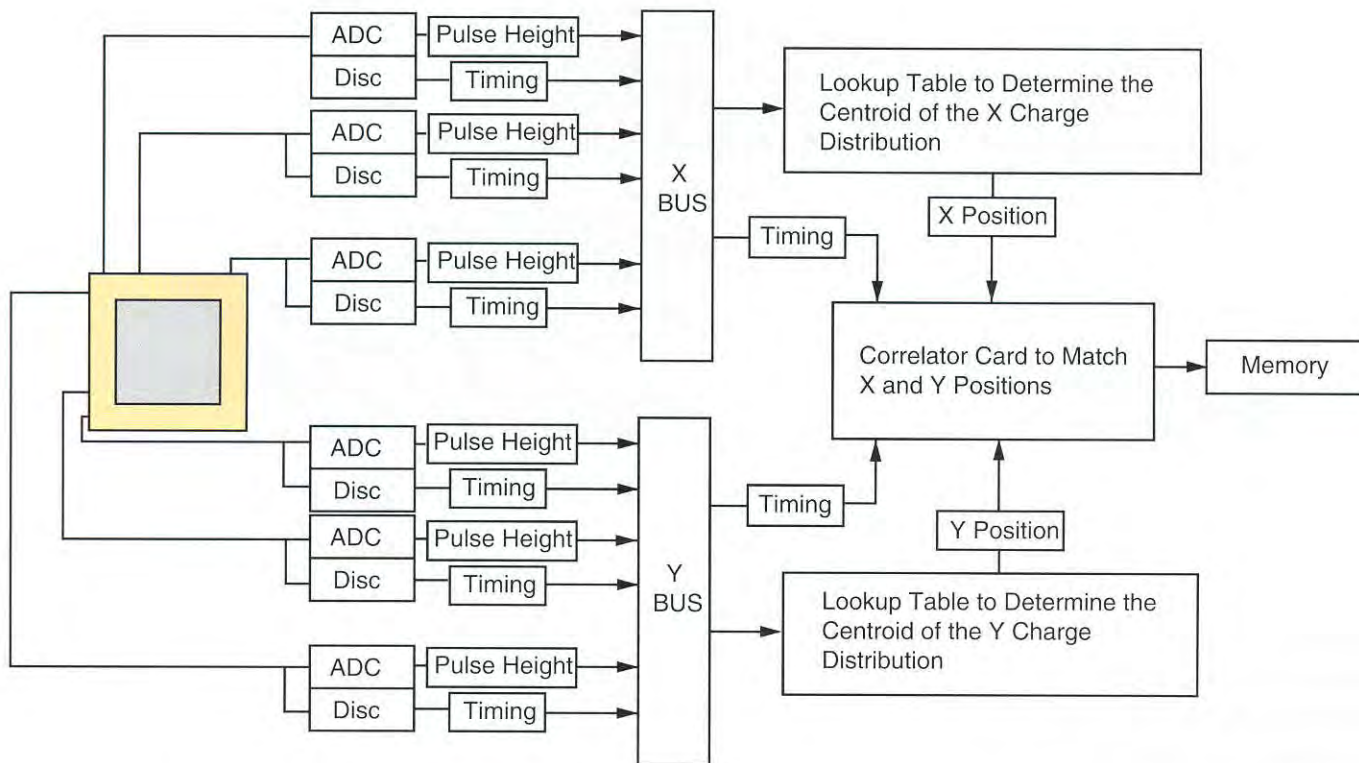


Figure 2 Block diagram showing the block structure of the fast 2 dimensional data acquisition system. The system has a master clock of 160 Mhz

four wires most closely surrounding an X-ray interaction are used to calculate the position of the event by interpolation.

The system has been designed to accommodate 256 channels in each dimension but cost constraints have limited the current system to 128x128 channels. The core of the system is contained in two 2m high racks, one for each dimension, and consists of nineteen printed circuit boards which have 18 layers and are 0.5m high. It is controlled by three VME computer systems and a fully populated system dissipates 8kW with each rack requiring water cooled heat exchangers. The multi-channel data acquisition system is capable of counting in excess of 2×10^7 photons/sec.

3) A fast histogramming memory system (DL200)

The Daresbury DL200 memory system which has been in routine use for a number of years with the delay line systems is one of the fastest large capacity histogramming memory systems in the world. It has a maximum capacity of 4Gbytes but its rate performance is limited to $\sim 5 \times 10^6$ counts/sec for extended periods, which is some four times slower than the expected performance of RAPID. The output of the RAPID system therefore produces four parallel data streams into four DL200 systems. The

upper bits of the memory address-word can be selected to represent time frames, if time resolved imaging is connected to it. The memory is dual ported, so the images can then be addressed by normal VME software to produce a real time display.

SRS Test results

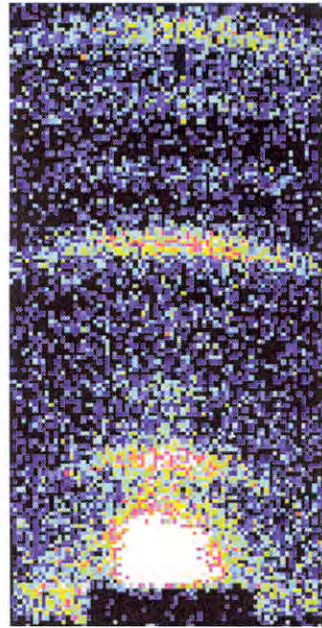
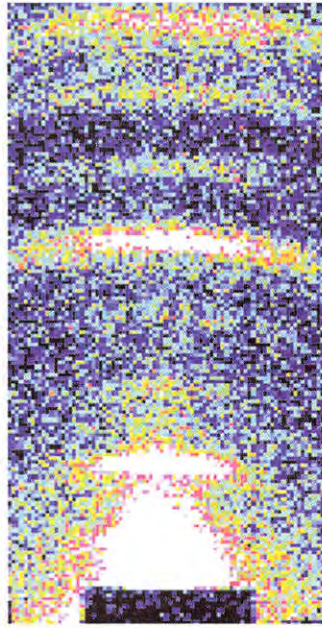
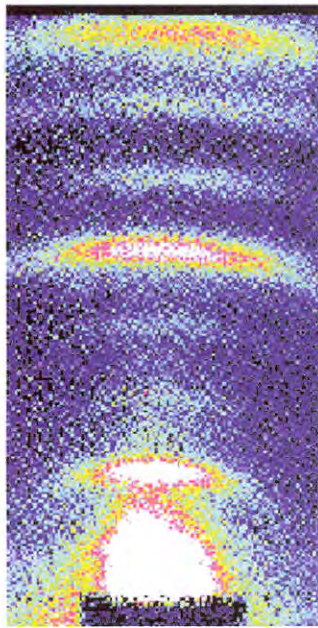
Tests of a subset of the RAPID system have very recently been carried out on the SRS station 16.1. Only six ADC boards were fully commissioned and so the system consisted of 64x32 channels covering an active area of 64x32mm.

Three detector systems, RAPID, a delay line area detector and an image plate were used to record various diffraction images at a camera length of 2.5m and an X-ray energy of 8.9keV. The maximum count rate that we were able to achieve using a polymer sample into a $60 \times 30 \text{mm}^2$ area, which included the very intense region surrounding the beam stop, was 2.7×10^6 photons/sec. Fortunately, this rate corresponds to a rate of $\sim 2 \times 10^7$ photons/sec over the full system of 128x128 channels. As RAPID is a parallel system in which the rate performance scales with the number of channels, this represents a very realistic test of the rate capability of the system. The system proved capable of handling the maximum count rate that could be produced on 16.1 with no

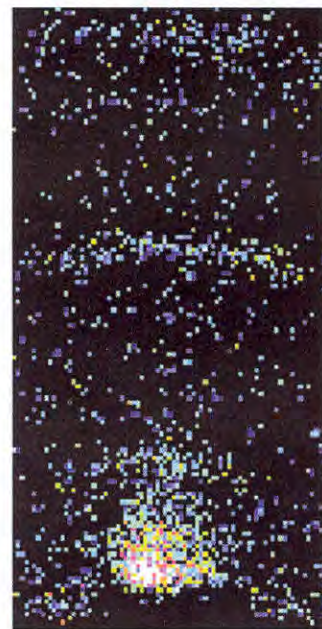
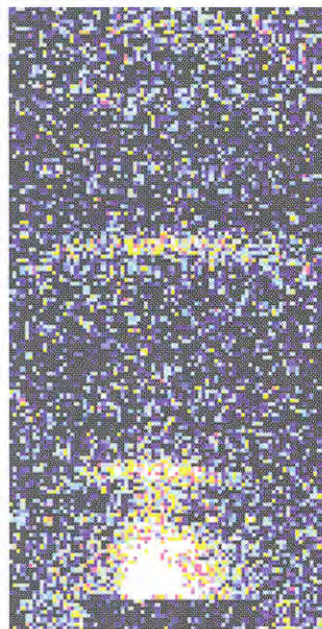
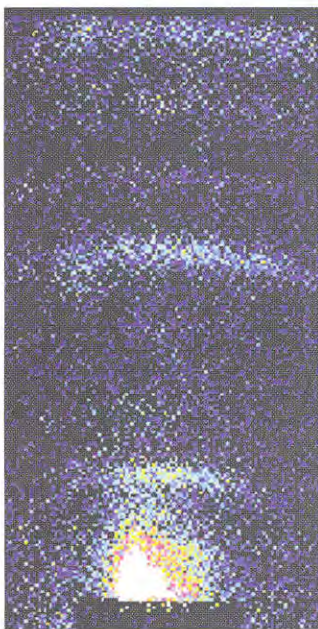
RAPID Detector
No attenuation

Image Plate
No attenuation

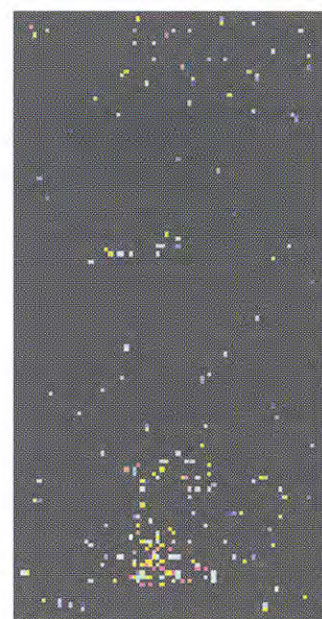
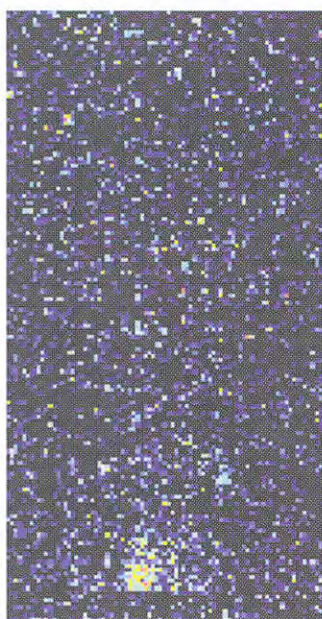
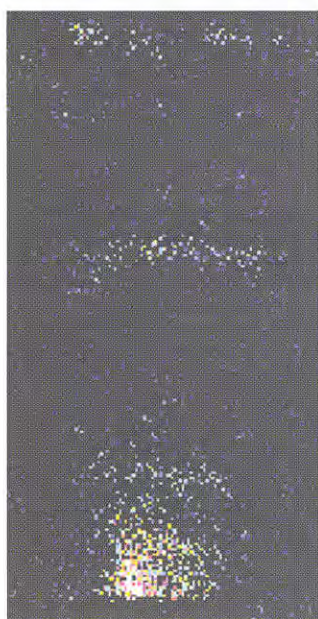
Delay Line Detector
9x attenuation



1 sec



100 ms



10 ms

Figure 3 Diffraction images of dry rat tail collagen taken on the three detectors at three exposure times.

attenuation at all. In contrast, the delay line detector required a 9x attenuator to be inserted in front of it, to reduce the count rate to a level which it could handle. The image plate of course required no attenuation.

Figure 3 shows diffraction images of dry rat tail collagen taken on the three different detector systems at 3 exposure times. The signal to noise in the RAPID images is clearly superior to that from the other 2 detectors with the 3rd, 6th and 9th order reflections being visible even from a 10ms single shot. The noise level of the image plate obliterates everything in the 10ms exposure whilst the 9x attenuator in front of the delay line detector means that there are insufficient photon statistics to make out any reflections.

During the tests, various problems with the RAPID system were identified. One of these problems can be seen in the intense part of the images where some structure is apparent which is not seen in the image plate data. This structure is caused by an under optimization of the interpolation algorithm which was used for these tests because there was insufficient information to perform the optimization. Now that we have a fully working system, we are confident that this can be corrected.

Conclusions

RAPID works and produces high quality 2-D images at a significantly higher rate than is possible with existing photon counting detectors. It is capable of handling unattenuated diffraction from the SRS from both polymers and biological samples and its noise performance is very much better than an image plate. The electronics commissioning is almost complete and the racks and cooling system are working well. The prototype MicroGap detector with active area of 128 x 128 mm is fully commissioned and working satisfactorily and a new 200 x 200mm active area detector with 128 x 128 electrodes is under construction.

Several difficulties have been identified and further work remains to be done. The calibration and interpolation algorithms must be optimized and system performance tests and characterisation performed. The 4 way striping of the memory system has to be implemented and the user software needs to be completed and debugged.

After completion of the system, integration with the

large area high pressure [3] technology will produce a high rate parallax reduced system for high angle diffraction.

References

- [1] R.A. Lewis, C. Hall, B. Parker, A. Jones, W. Helsby, J. Sheldon, P. Clifford, M. Hillen. *N. Fore. Nucl. Instrum. & Meths. A* (in press)
- [2] R.A. Lewis, N. Fore, W. Helsby, C. Hall, A. Jones, B. Parker, I. Sumner, J.S. Worgan, C. Budtz-Jørgensen (1992) *Rev. Sci. Instrum.* **63(1)**, 642-647
- [3] F. Ortuno-Prados, C.J.Hall, W.I. Heslby, A.O. Jones, R.Lewis, B. Parker, J. Sheldon *Nucl. Instrum. & Meths. A* (in press)

Neutron Diffraction Study of B-DNA Hydration

L.H.Pope¹, M.W.Shotton¹, V.T.Forsyth¹, P.Langan², H.Grimm³, A.Rupprecht⁴, R.Denny⁵ and W.Fuller¹

¹ Physics Department, Keele University, Staffordshire, ST5 5BG, U.K.

² ILL, Grenoble, France

³ Institute für Festkörperforschung, Jülich, GmbH

⁴ Arrhenius Laboratory, Stockholm University, Sweden

⁵ CCLRC Daresbury Laboratory, Daresbury, Warrington, U.K.

A high angle neutron fibre diffraction study of the distribution of water around the B conformation of DNA has been carried out using the D19 diffractometer at the ILL, Grenoble. Datasets were recorded for DNA in both a D₂O and H₂O environment. Various data analysis techniques involving CCP13 software have been exploited to generate Fourier maps which show the water distribution around the DNA. An ordered water network has been observed in both the major and minor grooves. Refinement of these water positions is revealing a detailed picture of the hydration of this particular conformation.

Introduction

Understanding the structure and hydration of DNA is biologically extremely important. For example it has been shown that water molecules within the groove of the double helix stabilise protein-DNA interactions involved in the regulation of gene

expression. The conformations that the DNA double helix can adopt depend primarily on base pair sequence, hydration and ionic environment. Determination of the hydration network of a particular DNA conformation will hence reveal important information about the role that H₂O plays in structure stabilisation.

Determining DNA structures and the location of interacting cations has been successfully achieved using X-ray fibre diffraction techniques. However these techniques have proved to be less suitable for locating positions of water molecules involved in the stabilisation of DNA conformations. Neutron fibre diffraction was developed as a technique to locate these water positions. The technique is based on the ability to isotopically replace H₂O by D₂O. The large difference in scattering powers of the two hydrogen isotopes can be used to generate difference Fourier maps showing the locations of the water molecules.

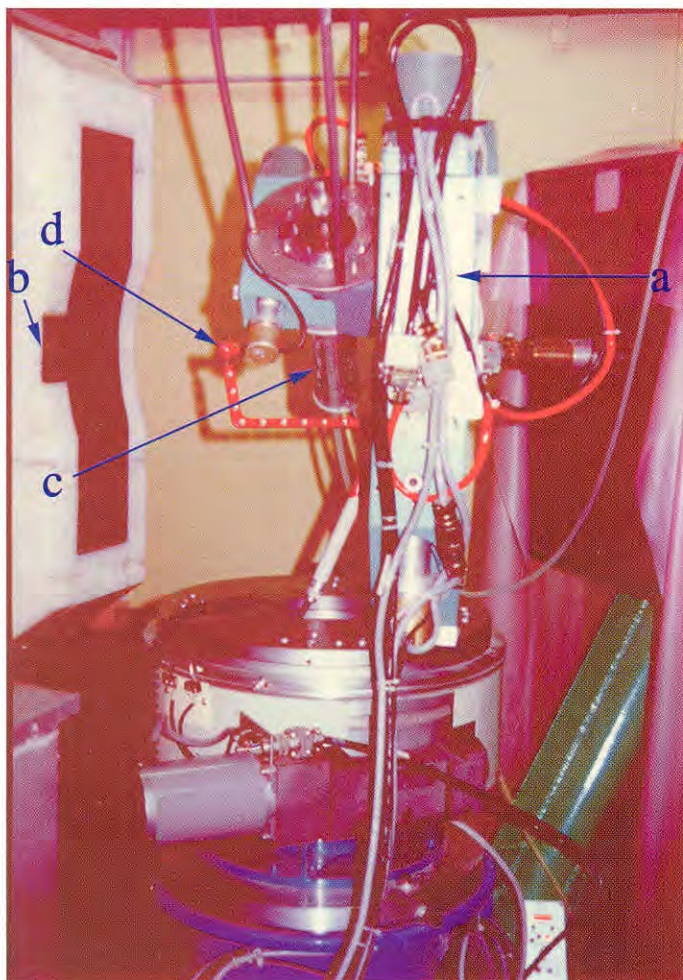


Figure 1: A photograph of D19 showing the four circle diffractometer, the gas filled curved position sensitive detector and the sample can designed to obtain either a H₂O or D₂O sample environment at the required humidity. The sample is positioned inside the can and is attached to the diffractometer using a goniometer mount. The components are indicated as follows: (a) four circle diffractometer, (b) detector, (c) sample can and (d) backstop

Fourier synthesis maps of the DNA + D₂O data also successfully reveal water positions and have the added advantage that they are computed from data where incoherent background scattering from hydrogen is minimised. Previous neutron diffraction experiments have used isotopic difference Fourier techniques to locate the water positions around the A-DNA and D-DNA helices.

In contrast to previous DNA neutron fibre diffraction experiments, there were two new features concerning data acquisition.

(1) A wet spun film sample, with dimensions ~2cm x 2cm x 0.75mm was used. The quality of the sample was excellent in both orientation and crystallinity. Previous experiments were carried out using samples prepared from single fibres arranged in a parallel array.

(2) Fibre precession geometry was used. This method was devised in order to optimise the efficiency of the data collection process and also to fill in the "blind region" parallel to the fibre axis [1]. D19's 4 circle diffractometer was used to vary the geometry of the sample position relative to both the neutron beam and the gas-filled position-sensitive detector. Figure 1 shows a photograph of the experimental set up on the D19 instrument.

Sample Preparation

The film sample used was prepared using the "wet spinning" method as devised by A. Rupprecht [2]. The wet spinning technique involves the extrusion of DNA, using an automated syringe, through a spinnerette into an alcoholic solution. This causes the formation of threads of DNA which are then wound onto a teflon coated cylinder which has both axial rotation and translation movement. The DNA is then cut from the cylinder and the sheet bathed in ethanol with the required salt content. For the crystalline B conformation the sheet was prepared using calf thymus DNA in a high concentration lithium salt environment.

Data Collection

The data were collected using a curved position sensitive detector, with an aperture of 64° by 4°. Two datasets were recorded, firstly with the DNA in a H₂O environment and then in a D₂O environment. The diffraction patterns obtained consisted of a series of 64° x 4° strips, each strip with a 1° overlap in order

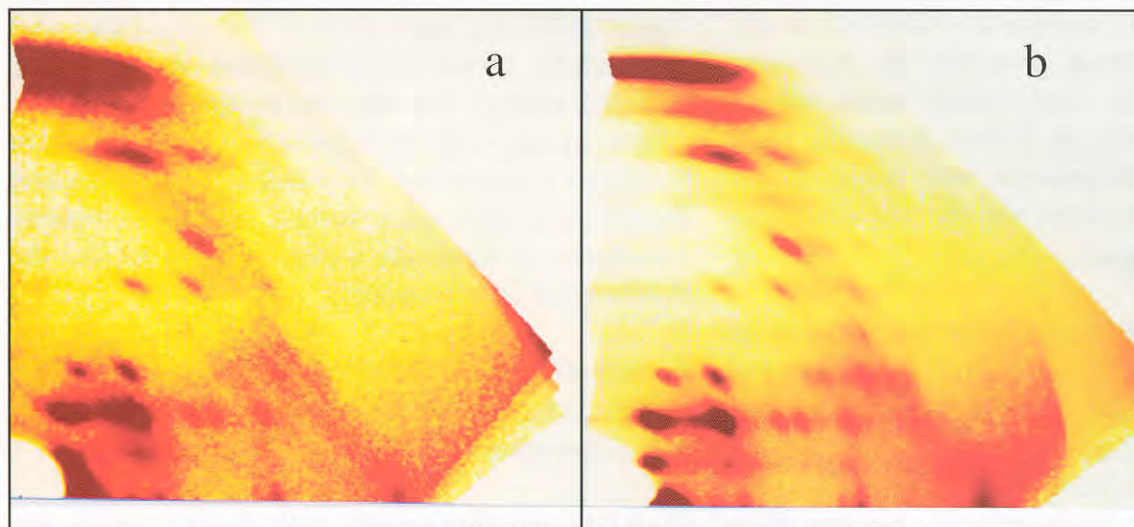


Figure 2 (a) The H₂O data set, comprised of four different sample orientations, mapped into reciprocal space. (b) A continuous LSQINT fit to the data.

to avoid edge effect errors in the final image. The fibre precession technique was used which involved the collection of data with the film sample at four unique orientations relative to the incident beam and the detector. These orientations correspond to four separate fibre tilt angles and therefore allowed the blind region around the (0,0,10) to be filled in.

Data Analysis

Software developed for D19 was used to correct for detector response and map the data into reciprocal space. A correction was applied to the data to account for the effects of absorption by the sample. CCP13 software was next used in order to measure the relative intensities of the diffraction maxima [3]. For comparison two independent methods were used:

(1) LSQINT with the Bragg fitting option and the roving window method for background calculation was used to measure the data. Due to the poor statistics of neutron data, generating a good fit was difficult. In order to eliminate the generation of additional peaks, which were not present in the raw data, LSQINT was modified so that it only fitted peaks to given h,k,l values.

(2) A continuous LSQINT fit to the data was generated and measured using a program which had FIT incorporated within it. This enabled us to interactively measure the intensities of the peaks and assign the intensity to the desired lattice indices. It can be seen from figure 2 that the method provided an excellent fit to the observed data.

The B form of DNA packs into an orthorhombic lattice in space group P2₁2₁2₁ having parameters $a = 30.8\text{\AA}$, $b = 22.5\text{\AA}$ and $c = 33.8\text{\AA}$. A molecular model

was generated using the atomic coordinates published by Arnott and Hukins [4] from which structure factor amplitudes and phases were calculated. The phases for the B model with exchangeable hydrogens replaced by deuterium were



Figure 3: The above photograph shows the B-form model with refined water positions in the major and minor grooves. The major groove positions can be seen as blue stippled spheres and the minor groove positions as purple spheres.

used as starting phases for the D₂O dataset, which enabled the generation of a Fourier synthesis map. In addition to the density associated with the DNA model itself, peaks were identified with D₂O around the molecule. These positions were refined and then included in the model and hence used to generate a new set of phases and a new synthesis map. Figure 3 illustrates the initial refined positions that were chosen in both the major and minor grooves. Repeating this procedure of phase and position refinement is allowing an accurate model of the B-DNA plus hydration to be constructed. A difference Fourier map of $F_{\text{DNA+D}_2\text{O}} - F_{\text{DNA+H}_2\text{O}}$ amplitudes was used as a comparison to the DNA + D₂O Fourier synthesis.

Results

The two Fourier maps generated from the continuous and Bragg fit to the data were virtually identical. This was encouraging as using a continuous fit to measure Bragg data could be useful for measurement of poorly observed data in the future. The Fourier difference map was found to be in good agreement with the Fourier synthesis map. Both maps showed extensive major and minor groove hydration. In

particular close interactions of the water between the sugar oxygen and the N3 of purine bases or the O2 of pyrimidine bases in the minor groove were observed.

Discussion

Neutron diffraction experiments of DNA require very large volume samples. Samples containing individually prepared fibres or those obtained by wet spinning are ideal. Results from neutron high angle fibre diffraction studies can be compared with results from single crystal X-ray diffraction experiments on short oligonucleotide duplexes. Whilst these single crystal experiments typically offer atomic resolution, care must be taken in extrapolating the results to the continuous polymer, since the influence of end effects in the oligonucleotide and crystal packing forces must be considered.

The neutron fibre diffraction study described clearly provides information relating to the extended polymer. However, in this case the data are sequence averaged since random sequence calf thymus DNA was used. The positions which have so far been identified occur in an environment which is relatively independent of base sequence. Any sequence-dependent water interactions are expected to be observed at much lower intensity due to averaging. For example, single crystal studies of the hydration of B-DNA have revealed a minor groove spine of hydration which is disrupted by G-C sequences [5]. Future neutron fibre experiments involving the study of the B conformation of specific base sequences will be of significant interest. Of particular interest will be the effect that extended G-C sequences have on the minor groove spine of hydration.

Future Work

Recent x-ray diffraction studies revealed that the sample exhibited double orientation and so in order to collect a much more detailed diffraction dataset the sample had to be rotated about its meridian and data collected at each sample rotation. This experiment has been performed on instrument D19 at the ILL, Grenoble. The sample was mounted on the diffractometer with its meridian aligned with the diffractometer phi axis. Phi was then incremented to provide sample rotations from -60° to +60° in steps of 10°, with data being collected at each phi. The 10° increment was considered an adequate sampling interval for the Bragg reflections which exhibited

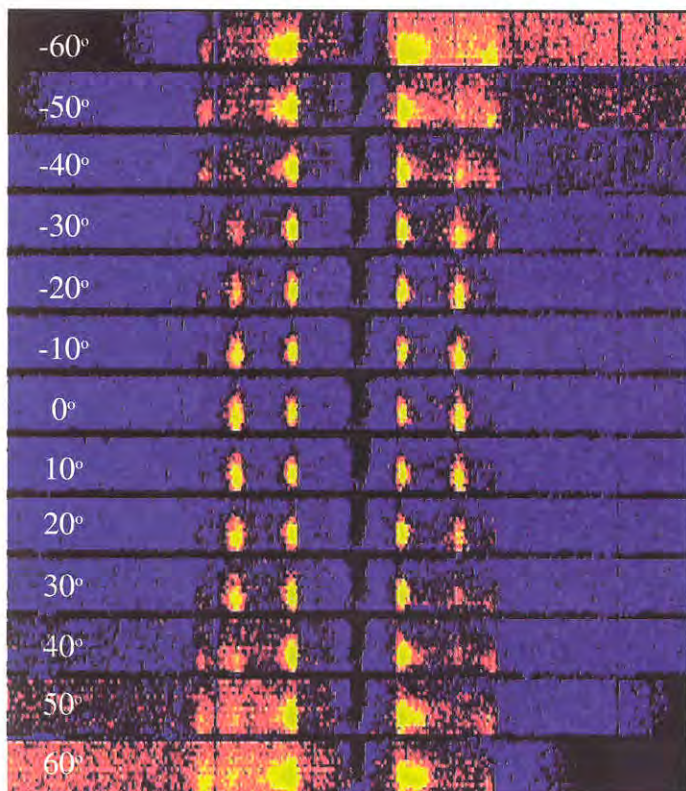


Figure 4: Recent equatorial data collected on D19 illustrating the double orientation of the sample. Each frame corresponds to a different phi rotation about the c axis as labelled above. A number of reflections can be seen coming on and off the Ewald sphere.

angular widths of approximately 60° . In order to collect a complete diffraction dataset a range of rotation of 180° was required. Physical sample restrictions limited data collection to a range of 120° but due to the large angular width of the reflections, reciprocal lattice points occurring in the 'physical blind region' had associated reflections which were visible within our range of rotation and could be fitted by extrapolation of the recorded data. Figure 4 shows data collected on the equator at sample rotations ranging from -60° to $+60^\circ$ in increments of 10° . The data recorded during this neutron fibre diffraction experiment are in the process of analysis at the present time. The data recorded are expected to reveal a more detailed picture of B-DNA hydration.

References

- [1] Langan, P., *et al*, *J. Appl. Cryst.*, (1996) (in press)
- [2] Rupprecht, A., *Biotech. Bioeng.*, **7**, 93, (1973)
- [3] Denny, R.C. (in preparation)
- [4] Arnott, S., Hukins, D.W.L., *Biochemical and Biophysical Research Communications*, Vol. **47**, No. 6, 1504-1510, 1972
- [5] Drew, H.R., Dickerson, R.E., *J. Mol. Biol.*,

Chain Conformations in Polyurethanes : A SAXS & SANS Study

A.J. Ryan^{1,2}, S. Naylor¹, N.J. Terrill¹, S. King³

1 UMIST Materials Science Centre
 2 CCLRC Daresbury Laboratory
 3 CCLRC Rutherford Appleton Laboratory

Segmented polyurethanes are statistical block copolymers comprising incompatible hard and soft blocks. A range of poly(ether-urethane) copolymers have been synthesised in order to verify which is the primary driving force behind microphase separation: block incompatibility or crystallisation of the segments. Two classes of copolymer have been synthesised: one class contained a semi-crystalline 4,4'-methylene diphenyl diisocyanate (4,4'-MDI) and butanediol (BDO) based hard segment, the other contained an amorphous hard segment based on a blend of 2,4- and 4,4'-methylene diphenyl diisocyanate (2,4/4,4'-MDI) and BDO. The soft segment in both types of copolymer was polypropylene oxide (PPO). The materials were synthesised with various hard segment contents: 25, 50 and 75 % by weight. The PPO samples had

molecular weights that ranged from 400 to 4000. Characterisation of the materials involved heating the materials until homogeneous in order to remove all traces of prior thermal history, and then annealing the samples at different temperatures. Quenching in liquid nitrogen was used to "freeze-in" the resultant morphologies. These samples were then analysed using separate differential thermal analysis experiments (DTA) and X-ray scattering experiments. Both the 4,4'-MDI and 2,4/4,4'-MDI copolymers which contained low hard segment contents or low molecular weight soft segments were shown to be homogeneous after annealing. Annealing had little effect on these materials. However, annealing the higher molecular weight 4,4'-MDI copolymers promoted crystallisation and produced larger microdomains with sharper interfaces. As a consequence of this, the PPO chains were stretched more in the 4,4'-MDI copolymers than in the 2,4/4,4'-MDI materials. In contrast, annealing had little effect on the 2,4 / 4,4'-MDI copolymers, evidence that crystallisation plays an

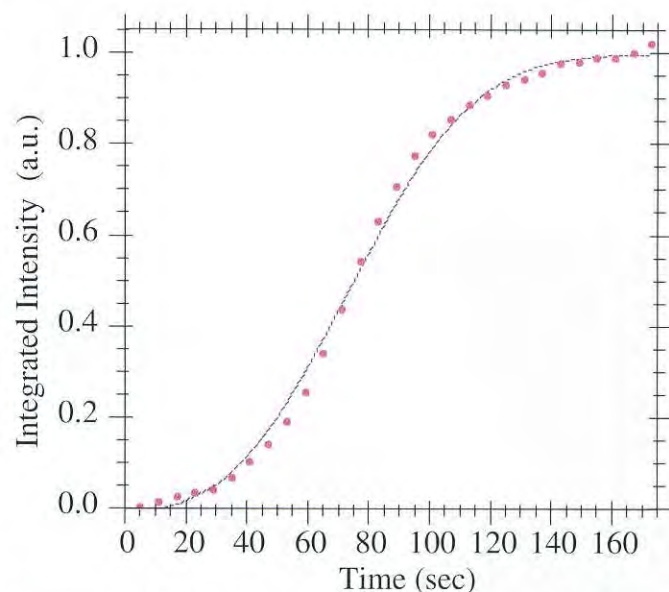


Figure 1 Integrated intensities during the isothermal microphase separation of a polyurethane. The line is a fit of the Avrami model to the data.

important part in the microphase separation process. The kinetics of microphase separation and crystallisation were investigated using time-resolved X-ray scattering experiments. Several models were used, including Avrami and time-dependent Ginzburg-Landau (TDGL) analysis. Aspects of the microphase separation process fitted both the spinodal decomposition (SD), and nucleation and growth (NG) models. However, the latter was favoured because the Avrami equation was seen to be in excellent agreement with the data (see Figure 1),

and fitted the data better than the SD models. The thermal history of the 4,4'-MDI materials was observed to have an important effect on the melting behaviour of the samples, possible causes being chain branching and side-reactions.

Changes in the conformation of the PPO soft segment were investigated using small-angle neutron scattering (SANS). A phase contrast matched copolymer was used to measure changes in the radius of gyration of the soft segment with temperature in a semi-crystalline, microphase-separated material. The Debye model fitted the data well (see Figure 2), and showed the soft segments to be initially in somewhat extended conformations, as a result of chain stretching brought on by movement of the hard

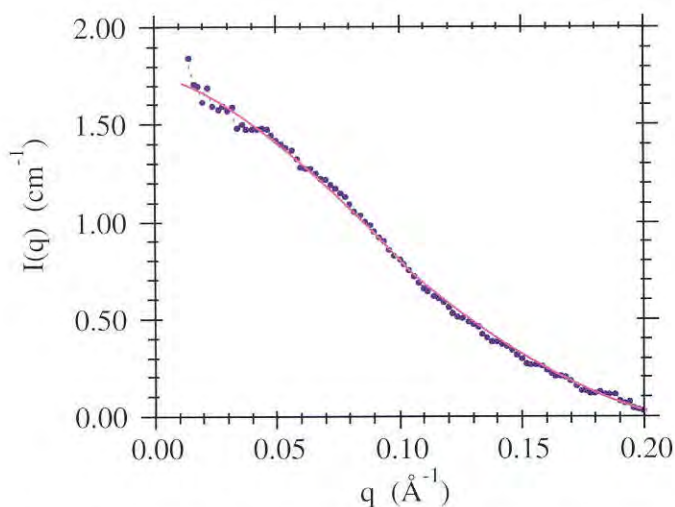


Figure 2: Fit of the Debye Model to the SANS data for a contrast matched material.

segments during microphase separation / crystallisation.

On heating, some disordering occurred as the soft segments began to pull hard segments out of the domains, to take the form of random coils. In addition, SANS patterns from hydrogenous polymers showed excellent agreement with SAXS patterns, confirming that the microdomains present in the microphase separated materials were the scattering entities in both techniques, and provided confidence in the spatial information so obtained.

Changes in the long period, obtained using correlation function analysis on SAXS data for a hydrogenous copolymer, correlated well with changes in the SANS data obtained for the contrast matched equivalent. The sample was shown to begin to disorder on softening at $\approx 100^\circ\text{C}$ and was mostly phase mixed by 180°C with some isolated crystalline

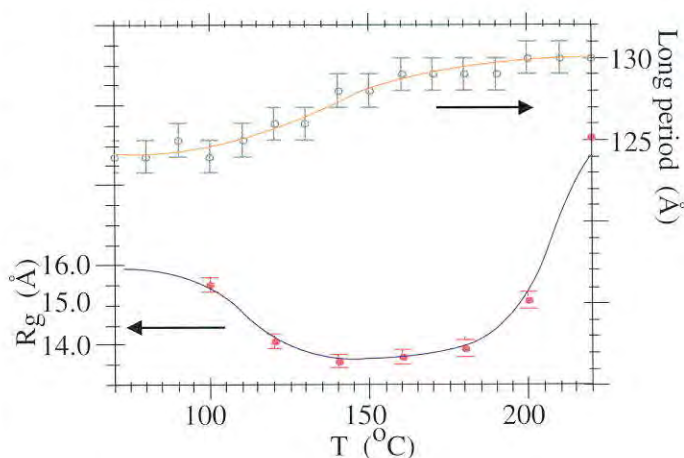


Figure 3: Variation in the long period, from SAXS, and the R_g of the soft segment, from SANS, as a function of temperature.

domains present. At $\approx 200^\circ\text{C}$ these larger domains melted as the material became homogeneous. As the temperature is increased, the radius of gyration of the soft segment initially decreases. This occurs because the retractive forces exerted by the soft segment increase with temperature, and consequently pull some hard segments out of the hard domains, so that the soft segments relax into smaller random coils. At higher temperatures, phase mixing begins to take place, leading to an increase in R_g as a result of interactions between the hard and soft segments, much as a homopolymer is swollen by a good solvent. The segments still take the form of random coils but are somewhat extended. The long period spacing L_p increases steadily with temperature once the material begins to soften at $\approx 100^\circ\text{C}$, until a temperature of 160°C is reached, when the long spacing remains relatively constant at 129\AA . This behaviour may be attributed to the preferential melting of smaller crystalline domains: hard blocks containing a lower number of MDI-BDO residues will begin to melt first, from simple thermodynamic considerations. As these hard blocks melt, the soft segments attached to them will relax into random coils, and this is reflected in the observed decrease in R_g . At this point the sample resembles a mixed phase matrix with isolated large crystalline domains distributed throughout, *i.e.*, the sample is mostly disordered but retains some crystallinity. A further increase in L_p and R_g is observed at $\geq 200^\circ\text{C}$, when the remaining hard domains begin to melt.

The experimental studies confirmed the domination of crystallisation over microphase separation due to

Structural Studies of Helical Poly(β -L-Aspartate)s

C.Aleman, F.Lopez-Carrasquero, J.J.Navas,
M.Garcia-Alvarez, S.Leon and S.Munoz-Guerra

Department d'Enginyeria Quimica, E.T.S.I.I.B., Universitat
Politecnica de Catalunya

Poly(β -L-aspartate)s are nylon 3 derivatives with an alkoxy carbonyl group stereoregularly attached to the backbone β -carbon atom of every repeating unit: $[\text{NHCH}(\text{COOR})\text{-CH}_2\text{-CO-}]$. This family of compounds is able to crystallise in helical structures with features similar to the α -helix characteristic of polypeptides. More specifically, poly(α -isobutyl- β -L-aspartate) constitutes the first example of a nylon derivative taking up helical conformations traditionally restricted to polypeptides and proteins [1]. On the other hand, it is a well known feature that in polypeptides, in particular in poly(β -alkyl- α -L-aspartate)s, minor modifications in the side chain may give rise to changes in the conformational parameters or may even reverse the handedness of the helix [2]. Consequently, a detailed study of the influence of the side group R on the helical structures of poly(β -L-aspartate)s is highly desirable.

In this work we examined the helical structures of six polymers:

- I. poly(α -methyl- β -L-aspartate);
- II. poly(α -ethyl- β -L-aspartate);
- III. poly(α -propyl- β -L-aspartate);
- IV. poly(α -n-butyl- β -L-aspartate);
- V. poly[α -(2-methoxyethyl)- β -L-aspartate];
- VI. poly(α -cyclohexyl- β -L-aspartate).

The crystal structures of such compounds were characterised by X-ray diffraction of fibres and films. Molecular models corresponding to such structures were determined by combining two well-established methodologies. Firstly, a conformational analysis using energy calculations was performed in order to find the more favourable molecular models. Secondly, such models were refined against X-ray diffraction data with the Linked-Atom Least-Squares (LALS) methodology.

A hexagonal crystal form was found for the six compounds under study. It is composed of 17/4-helices for the methyl and ethyl derivatives and of 13/4-helices for poly(β -L-aspartate)s with medium

size side groups. In all cases the helices are right-handed and the chains are arranged in anti-parallel. A second crystal form was found for the ethyl, propyl and n-butyl derivatives. This is a tetragonal structure which consists of a parallel arrangement of 4/1-helices. In spite of the structural variability with the size of the side group, a feature general to the whole family of these polyamides can be concluded from this work. Thus, it may be stated that all the helical structures of poly(β -L-aspartate)s are composed of right-handed helices stabilised by intramolecular hydrogen bonds.

References

- [1] Fernandez-Santin, J.M.; Aymami, J.; Rodriguez-Galan, A.; Munoz-Guerra, S.; Subirana, J.A. *Nature* (London) 1984, **311**, 53.
- [2] Fraser, R.D.B.; MacRae, T.P. in "Conformation in Fibrous Proteins", Academic Press, New York, 1973.

X-Ray Diffraction From Branched Polyethylenes: Evidence for a Partially Ordered Component

A.M.E.Baker and A.H.Windle

Department of Materials Science and Metallurgy, University of Cambridge, Pembroke Street, Cambridge, CB2 3QZ.

We have examined fifteen samples of commercial branched polyethylenes by powder and fibre diffraction. The fibre diffraction was recorded from a novel fibre diffractometer based on a scanning CCD camera, recently designed and built in our department [1]. The diffraction patterns were fitted using the CCP13 suite of programs for the fibre data and the Rietveld method for the powder data. Fitting to the whole pattern was dominated by the two intense lowest angle reflections, (110) and (200) and produced a poor fit to the higher angle reflections. Separating each pattern into a low angle region containing (100) and (200) and a high angle region containing all other reflections produced good fits; however, cell parameters from these were incompatible. The (110) and (200) reflections consistently occurred at lower angles than expected from the higher angle reflections. This discrepancy between the observed and calculated positions increased with higher levels of branching.

Polymers are traditionally viewed in terms of a crystalline and a non-crystalline component. It is

here hypothesised that the discrepancy between low and high angle regions was caused by the presence of a third component of intermediate order. The (110) and (200) reflections are then superimpositions of diffraction from this component and from crystalline material whilst the weaker higher angle reflections represent diffraction only from the crystalline material. Only lower angle reflections are expected from a less well ordered component because of the rapid attenuation in diffracted intensity caused by the high levels of structural disorder and distortion. Our data are consistent with the additional component representing the surfaces of crystallites and possibly containing a relatively high concentration of branches because of rejection from the crystallites. An interfacial component has been proposed in polyethylene by other experimental techniques, most notably Raman spectroscopy [2], although the interpretation of these results is currently a matter of fierce debate [3,4].

References

- [1] Hanna, S. & Windle, A.H. (1995). *J. Appl. Cryst.* **28**, 673-689.
- [2] Shen, C., Peacock, A.J., Alamo, R.G., Vickers, T.J., Mandelkern, L. & Mann, C.K. (1992). *Appl. Spectroscopy* **46**, 1226-1230.
- [3] Naylor, C.C., Meier, R.J., Kip, B.J., Williams, K.P.J., Mason, S.M., Conroy, N. & Gerrard, D.L. (1995). *Macromol.* **28**, 2969-2978.
- [4] Mandelkern, L. & Alamo, R.G. (1995). *Macromol* **28**, 2988-2989.

Micro-diffraction on Keratin Fibres

B. Busson, F. Briki and J. Doucet

LURE batiment 209D, Centre Universitaire Paris-Sud, 91405 ORSAY Cedex, FRANCE

Interest of keratins

The word α -keratins [1] is used to name a group of proteins which show a high degree of sequence homologies and common structural features. They are the main component of hair, wool, epidermis, feathers, nails and quills, and play a major structural role in all animal and human tissues, owing to their high durability and outstanding physical properties. Therefore, they are involved in textile, pharmaceutical and cosmetic industries.

General presentation of the study

Keratins are usually classified into four groups according to their X-ray diffraction pattern: α (e.g.

hair), β (stretched hair), feather and amorphous [1,2]. But this simple classification does not take into account that various types can co-exist in the same tissue and that modifications of the external or mechanic conditions can induce transitions from one type to another, for instance the α Δ β transition observed on stretching a hair [3]. Up to now the internal organisation inside the fibres is not well known.

We are presently trying to improve our knowledge of the molecular and supramolecular organisation of keratin fibres and in particular the understanding of the α to β transition. We are deriving a model of keratin packing through X-ray diffraction data from various keratins (horsehair, porcupine, hair, feather, wool...) obtained in various humidity, temperature and mechanical conditions.

Micro-diffraction experiments

We have performed wide angle micro-diffraction at the ESRF on beamline BL1-ID13 with a two microns diameter beam; we have obtained diffraction patterns from various samples (hair, horse hair, porcupine quills, stratum corneum and feather) and followed their evolution as a function of the depth from the surface.

We have thus recorded separate images from the amorphous outer layers (cuticle) and the cortex of the fibres, and seen the transition between these two zones; in addition, we have observed that the fibre direction varies with the distance to the surface for two-dimensional samples (porcupine, feather shaft) contrary to what is observed for unidimensional ones (hair, horse hair). Unfortunately, it has been impossible to perform SAXS experiments and to test the effect of stretching a hair on micro-diffraction patterns as a function of time.

New experiments are planned in order to get complementary results performing small angle micro-diffraction on our samples. SAXS experiments are necessary to complete our knowledge on the transition between the cuticle and the cortex; we would like to study the correlation between meridian and equatorial changes in the diagrams as the beam moves from the cuticle to the cortex. In addition, some characteristic reflections on keratin diagrams - most of which cannot be observed at wide angle - are supposed to be due to the cuticle only and we would like to separate them from the other ones.

Bibliography

- [1] Fraser, T.P. MacRae, G.E. Rogers "Keratins - their composition, structure and biosynthesis" Charles C. Thomas Editor (1972)
- [2] Garson, J. Doucet, J.L. LÈvÍque and G. Tsoucaris, "Oriented structure in stratum corneum revealed by X-ray diffraction" *J. Invest. Dermat.*, **96(1)**, 43-49 (1991)
- [3] Bendit "The alpha-beta transformation in keratin", *Nature*, **4558**, 553 (1957)

Real-Time Simultaneous SAXS and WAXS Measurements During Polymer Deformation

M.F.Butler¹, A.M.Donald¹, A.J.Ryan²

1 Cavendish Laboratory, University of Cambridge, Madingley Road, Cambridge, CB3 0HE

2 Manchester Materials Science Centre, Grosvenor Street, Manchester, M1 7HS

The usefulness of the simultaneous measurement of the two-dimensional small- and wide-angle X-ray scattering patterns in conjunction with the load-extension curve has been demonstrated using a wide variety of polyethylene (PE) samples. A comprehensive study of the influences of various structural parameters, such as molecular weight, percentage crystallinity, branch amount, size and distribution, has been performed in both tension and compression on unoriented bulk samples and in tension on oriented blown-film samples. Experiments have been performed over a range of strain rates and with slight modification of our commercially available deformation apparatus (Rheometrics Ltd Miniature Materials Tester), a range of temperatures (possible range from -60°C to +200°C).

Measurement of the load-extension curve with the SAXS and WAXS patterns has proved to be invaluable in relating the macroscopic to the lamellar and molecular deformation mechanisms. Selected results from a simple analysis of the evolution of the X-ray scattering patterns will be presented for PE. For the unoriented samples these will include demonstration of the correlation of the onset of a martensitic transformation (shown by WAXS), in which the stable orthorhombic unit cell is partially converted into a metastable monoclinic one, with the lamellar to fibrillar conversion (detected by a new meridional long spacing in the SAXS) and the macroscopic yield point in the load-extension curve.

Chain slip is shown to precede the martensitic transformation in compression but to activate at approximately the same extension in tension.

Results from an investigation of the deformation of rubber toughened PMMA will also be presented, in which the influences of the rubber particle concentration and crosslinking density in the rubber particles were studied. Cavitation and crazing mechanisms in the rubber particles and PMMA respectively have been identified from the SAXS patterns. Additional results, obtained at the ESRF, at very low scattering angles, have revealed the form factor of the rubber particles and the progress of deformation of the particles. Some other polymer systems studied by simultaneous SAXS/WAXS may also be discussed.

Crystallisation in Linear and Cyclic Poly (Ethylene Oxide): Implications for Chain Folding

J.Cooke¹ and A.J.Ryan¹, T.Sun², G.Yu², Z.Yang² and C.Booth²

1 Manchester Materials Science Centre, Manchester, M1 7HS, UK.

2 Manchester Polymer Centre, Department of Chemistry, University of Manchester, Manchester, M13 9PL, UK.

A series of specially synthesised poly(ethylene oxide) samples [1,2], has been used to make a comparative study of the molecular arrangement within equivalent cyclic and linear polymers. Such systems offer an opportunity to examine the nature of chain folding in normally helical chains. Both types of molecule are thought to crystallise as stacks with the long spacing of the linear samples being double that of the corresponding molar mass cyclic sample. Samples with molar mass ranging between 1000 and 10,000 g/mol have been produced.

High-frequency Raman spectroscopy has been used to define the molecular chain conformation and packing [3]. Measurements confirm that cyclic and linear chains crystallise in an identical manner, *i.e.* as alternate right and left-handed 7_2 helices aligned in stacks parallel to the fold plane, with the polymer chains defining a monoclinic unit-cell.

A time resolved X-ray scattering, SAXS/WAXS/DSC, developed at Daresbury Laboratory, Warrington, UK, has provided a method to further study the crystallisation behaviour of both linear and cyclic samples. Wide-angle diffraction patterns have been

collected from samples during melting and recrystallisation. The patterns indicate that the helical crystal structure is independent of molar mass and chain type (linear or cyclic).

Values of long spacing for each sample have been determined from small-angle patterns. Identical long-spacings have been observed from both linear and cyclic samples of equivalent chain length.

SAXS patterns collected from linear polymers with molar mass in excess of 4000 g/mol and the 10,000 g/mol cyclic polymer indicate that there is a transition from unfolded to folded-chain crystals at lower crystallisation temperatures.

Detailed studies of the enthalpy of fusion have been undertaken which allow the direct calculation of the surface free energy for PEO with chain folds.

References

- [1] Y.-Z. Yan, Z. Yang, C. Booth and C. Price, *Makromol. Chem., Rapid Commun.*, **14**, 725 (1993).
- [2] T. sun, G.-E. Yu, C. Price, C. Booth and A.J. Ryan, *Polymer Commun.* **36**, 3775 (1995).
- [3] K. Viras, Z.-G. Yan, C. Price, C. Booth and A.J. Ryan, *Macromolecules*, **28**, 104 (1995).

CCP13 Program Updates: A Graphical User Interface for Fit

R.C.Denny

Biophysics Section, Blackett Laboratory, Imperial College, London SW7 2BZ and CCLRC Daresbury Laboratory, Warrington, Cheshire WA4 4AD

The first graphical user interface (GUI) has been developed for a program in the CCP13 suite. XFIT is a Motif-based GUI developed using the UIM/X GUI builder for the peak fitting program FIT. This is an attempt to render the somewhat terse XOTOKO-style interface of FIT more friendly to new users and to lessen the key-pressing burden for the more experienced.

Other developments include modifications to FIX and FTOREC to take account of general detector orientation and the formulation of a particle orientation distribution function which is suitable for patterns where the degree of disorientation is high. This function is more flexible than those currently in use in LSQINT and should prove useful in all cases.

The Torus global optimization procedure will also be discussed.

Complex Melt Phases of PEO-PBO Diblock Copolymers

J.P.A.Fairclough¹, A.J.Ryan², I.W.Hamley³, S.Mai⁴, C.Booth⁴, B.Liao⁵ and R.C.Denny⁶.

¹ Materials Science Centre, UMIST

² Materials Science Centre, UMIST and CCLRC, Daresbury Laboratory

³ Department of Chemistry, University of Leeds

⁴ Department of Chemistry, University of Manchester

⁵ Department of Materials Science, Changsha Institute of Technology, Changsha, Peoples Republic of China

⁶ CCLRC, Daresbury Laboratory and Blackett Laboratory, Imperial College

Block copolymers are used in a wide variety of industrial and biomedical applications such as compatibilisers in polymer blends, surfactants and gelling agents in aqueous systems, viscosity modifiers in lubricating oils and texturisers in food [1-6]. Their useful properties stem from the tendency of the two blocks to microphase segregate. This gives rise to diverse structures. In the melt state, they form periodic ordered structures including lamellae, Ia3d gyroids, hexagonal cylinders and bcc spheres, as the volume fraction deviates from the 50/50 concentration. As the temperature is increased the ordered structure is destroyed and a disordered structure develops. At higher temperatures a mean field structure is seen.

The structures of the PEO-PBO diblock copolymer system were determined by SAXS/WAXS/DSC on Station 8.2 of the SRS at Daresbury. The results were analysed by the use of the FIT routine. The peak shape for the lamella morphology was seen to change from the Gaussian, instrument limited profile, at low temperature to a broad Lorentzian at high temperature above the ODT. The transition was seen to occur as a discontinuous jump at the ODT. Results will be presented for a range of morphologies including the lamella, hexagonal cylinders and the Ia3d structures.

References

- [1] Paul, D.R. in "Polymer Blends", Eds. Paul, D.R., Newman, S., Academic Press, New York, 1978, vol. 2
- [2] "Block Copolymers", Ed. Aggerwal, S.L., Plenum, New York 1970

- [3] "Developments in Block Copolymers-1", Ed. Goodman, I., Applied Science, New York, 1982
- [4] "Processing, Structure and Properties of Block Copolymers", Ed. Folkes, M.J., Elsevier, New York, USA, 1985
- [5] "Thermoplastic Elastomers", Eds. Legge, N.R.; Holden, G.; Schroeder, H.E., Hanser, New York, 1987
- [6] Brown, R.A.; Masters, A.J.; Price, C.; Yuan, X.-F. in "Comprehensive Polymer Science", Eds. Booth, C.; Price, C., Pergamon, Oxford, 1989, Ch. 6

Simultaneous Raman/SAXS/WAXS of Liquid Crystals and Polymers

H.F.Gleeson¹, G.Bryant¹, W.Bras², B.U.Komanscek³, N.McKeown⁴, A.Stennett¹, A.J.Ryan⁵.

1 Dept. of Physics and Astronomy, University of Manchester, M13 9PL.

2 AMOLF, Netherlands.

3 CCLRC Daresbury Laboratory

4 Dept. of Chemistry, University of Manchester, M13 9PL.

5 Manchester Materials Science Centre, UMIST.

Very recently it has been possible to carry out simultaneous SAXS/WAXS/DSC and Raman spectroscopy of advanced organic materials on station 8.2 at Daresbury, adding to the suite of simultaneous techniques possible. The use of several concurrent experiments allows the detailed determination of mechanisms involved in phase transitions and ordering phenomena in polymers and low molecular mass materials. This talk describes the addition of a Raman spectrometer to the existing SAXS/WAXS/DSC facilities and presents results for several of the systems studied. The presentation includes data for well known polymers, polymeric liquid crystals, and low molar mass materials, showing how the changes in molecular vibrations can be linked to ordering within the materials.

On the Shape of Transferrins in Solution

J.G.Grossmann and S.S.Hasnain

CCLRC Daresbury Laboratory, Daresbury, Warrington, Cheshire WA4 4AD, U.K.

Transferrins are key proteins of iron metabolism in mammals. The X-ray crystal structures of the primary members of the transferrin family (serum transferrin, lactoferrin and ovotransferrin) have now been determined [1] and revealed that the protein

consists of two homologous lobes, each of which binds one iron atom with high affinity. Both lobes can be further divided into two dissimilar domains. The essentially identical metal binding sites in both lobes lie in the interdomain cleft together with a bound synergistic anion, usually carbonate. X-ray diffraction [2] and solution X-ray scattering [3] studies on transferrins provided a major insight into the mechanism of metal binding and the concomitant large-scale movement of essentially rigid domains. Understanding the conformational changes that transferrins undergo upon metal binding is meaningful in elucidating their function. The molecule is able to perform a metal-induced large-scale conformational change by the wrapping of domains I and II in the N- and C-terminal halves, respectively, around the metal ion. The nature of the movement can basically be reduced to a rotation around a localised hinge [2].

The conformational difference between wide open and closed domains of transferrin is an issue of major concern in that it may be crucial in allowing access of the metal to the active site at the interface between the two domains, and in providing an efficient way of interaction with the transferrin receptor by discriminating a specific conformation, *i.e.* the iron-loaded compact closed state. High-resolution structures of lactoferrin [2,4] ascribe this flexibility which arises from a hinge-bending mode to low-energy deformations leading to a distribution of conformations in solution, a mechanism which is reminiscent of PacMan-like dynamics. In contrast, we show here that the open (iron-free) and closed (iron-loaded) structures are unique conformations of the protein under physiological conditions where the transition from open to closed state is stimulated by iron-binding in analogy to a Venus fly trap. This demonstrates that effects due to crystallisation conditions and/or forces in the crystal lattice must be responsible for trapped non-physiological configurations in the crystalline state.

We applied the model-independent approach using spherical harmonics [5] for the structural analysis of previously published synchrotron X-ray scattering data of the expressed native N-terminal fragment of human serum transferrin and one of its mutants (D63S) in the iron-free and iron-loaded state as well as of human diferric and apo serum transferrin [3]. Even though the nature of the scattering experiment implies the loss of structural information (regarding randomly distributed particles in solution and the

concomitant spherical averaging of scattering data), the direct shape determination using the available resolution regime in this study allowed a straightforward calculation of the protein surface.

References

- [1] Bailey *et al.* (1988) *Biochemistry* **27**, 5804-5812; Anderson *et al.* (1989) *J. Mol. Biol.* **209**, 711-734; Kurokawa *et al.* (1995) *J. Mol. Biol.* **252**, 196-207.
- [2] Anderson *et al.* (1990) *Nature* **344**, 784-787.
- [3] Grossmann *et al.* (1992) *J. Mol. Biol.* **225**, 811-819; Grossmann *et al.* (1993) *J. Mol. Biol.* **231**, 554-558.
- [4] Faber *et al.* (1996) *J. Mol. Biol.* **256**, 352-363.
- [5] Stuhmann (1970) *Acta Cryst.* **A26**, 297-306; Svergun & Stuhmann (1991) *Acta Cryst.* **A47**, 736-744.

Studies of Ceramic Formation

G.N.Greaves

CCLRC Daresbury Laboratory Warrington WA4 4AD

The processing of ceramics is generally played out, partly in alterations to the local environments of those impurities present (XAFS) that influence precipitation and partly in changes to the proportions of the various crystallographic protagonists (XRD) that ensue. Together this sequence of events contributes to the ensuing drama acted out on a larger scale as the characteristic microstructure (SAXS) is generated. XAFS, XRD and SAXS provide the essential combination of footlights needed to witness this complex theatre at all its various levels. Take cordierite whose crystallisation from cordierite glass precursors is denied when chromium is present as a nucleating impurity. On this occasion spinel is formed and intrigue is heightened by the arrival of another intermediate in the form of stuffed quartz - an aluminosilicate disguised as alpha SiO_2 . XAFS reveals the rogue aluminochromate that spawns the spinel. From XRD the sequence and development of both intermediates is clear, leaving SAXS the task of identifying the 20nm particle size (Guinier) and the evolution of 3 dimensional microstructure from an initial architecture that is distinctly fractal (Porod). Compared to the conventional disorder-order transition of ceramic processing, the collapse of a refined zeolite structure on annealing to an aluminosilicate glass is quite the opposite. The hallmark of this order-disorder transition is an uncanny switch in the Porod slope from ~ 3.5 to ~ 4 which

anticipates the crystalline demolition to follow and marks the onset of Euclidean geometry in the underlying microstructure. For what on the face of it is all but a transition from zeolite to glass, the maximum in the SAXS invariant pin points 50% crystallinity in the XRD zeolite peak heights (the Ryan trick) and by appealing to the Stroble & Schneider binary phase model the electron density contrast can be uncovered. This correlates with the change in fractal dimension to reveal a step-wise signature that is the same for zeolite A as for zeolite Y and may well be universal to the phenomenon of microporous collapse.

Molecular Conformations of Nitrogenase Studied by Solution X-ray Scattering

S.A.T.Haldane, J.G.Grossmann and S.S.Hasnain

School of Applied Sciences, De Montfort University, Leicester LE1 9BH, U.K. and CCLRC Daresbury Laboratory, Daresbury, Warrington, Cheshire WA4 4AD, U.K.

The enzyme nitrogenase catalyses the reduction of molecular nitrogen to ammonia in nitrogen-fixing micro-organisms. Nitrogenase consists of two metallo-proteins, the MoFe-protein (component 1) and the Fe-protein (component 2) which binds Mg-ATP. Their crystal structures from the species *Azotobacter vinelandii* (Av1 and Av2) and *Clostridium pasteurianum* (Cp1) have been determined recently and show that both are $\alpha\beta$ proteins. The Fe-protein is composed of two identical subunits connected by a 4Fe-4S cluster [1], while the MoFe-protein is an $\alpha_2\beta_2$ tetramer with structurally similar α and β subunits. Each $\alpha\beta$ dimer coordinates two types of metal centres: the FeMo-cofactor and the P-cluster pair [2]. Under molybdenum depletion and in the presence of vanadium, an alternative protein is expressed which contains V instead of Mo (VFe-protein) and at low levels of Mo and V an apparently iron-only protein (FeFe-protein) is expressed [3]. These alternative nitrogenases are expected to be similar to the MoFe-proteins. However, they have shorter β subunits that lack the N-terminal domain which wraps around the α subunits, and most intriguingly, there are two additional δ subunits, whose structure and function are unknown.

In order to define the overall molecular shape of component 1 proteins in the alternate nitrogenase systems in solution, we have been using the spherical

harmonics approach developed by Svergun & Stuhrmann [4]. The good quality scattering data on the MoFe protein from *Azotobacter vinelandii* (Av1) and *Klebsiella pneumoniae* (Kp1) have allowed us to determine the molecular shape in a model independent way. So far, the scattering data on the VFe protein of *Azotobacter chroococcum* (Ac1v) showed that this alternate nitrogenase seems to be less compact compared to Av1 and Kp1 with regards to its radius of gyration. However, its volume deduced from the scattering profile appears to be smaller compared to the Mo-based nitrogenases. This inconsistency led us to the assumption that the preparations of Ac1v did not consist of a monodisperse solution but rather a mixture of different conformations which makes the determination of the molecular shape of this non-molybdenum nitrogenase difficult. We were able to demonstrate that the metal-cofactors play an important role in the overall conformation of the protein.

We have adopted the same approach with the component 2, namely the iron protein which is expected to undergo a conformational change upon ATP binding. There is good agreement with the crystallographic structure for the native protein. However, our scattering experiments show a distinct difference from published data concerning Mg-ATP induced structural changes [5] even though further work is necessary to ensure that no ATP is present in the resting state. Interestingly in the crystal structure also, one of the two possible sites is occupied by nucleotide (1).

References

- [1] Georgiadis *et al.* (1992) *Science* **257**, 1653-1659.
- [2] Kim & Rees (1992) *Nature*, **360**, 553-560; Kim *et al.* (1993) *Biochemistry* **32**, 7104-7115.
- [3] Eady (1995) *Science Progress* **78**, 1-17.
- [4] Stuhrmann (1970) *Acta Cryst.* **A26**, 297-306; Svergun & Stuhrmann (1991) *Acta Cryst.* **A47**, 736-744.
- [5] Chen *et al.* (1994) *J. Biol. Chem.* **269**, 3290-3294.

The Crystallographic Binary File (CBF) Proposal

A.P.Hammersley

ESRF, BP-220, 38043 Grenoble Cedex, FRANCE

The "Crystallographic Information File" (CIF) is a standard throughout the international crystallographic community for electronic

transmission, submission, and archiving of structural data. CIF is maintained and developed by the COMCIF committee of the IUCr. Various extensions are being worked upon *e.g.* mmCIF for macromolecular crystallography, and powderCIF for powder crystallography.

In order to extend the CIF concept to cover storage of raw experimental data, and in particular "image" data, an e-mail discussion/working group, called "imageNCIF" has been formed. CIF is an ASCII text only standard, but pure ASCII encoding of large binary data-sets is felt to be inappropriate. Thus, the group proposes extending the CIF concept through a CIF-compatible header section stored within a binary file. This proposal is presently named the "Crystallographic Binary File" (CBF).

The technical issues involved in establishing a world-wide standard file format for raw experimental image data will be discussed, along with the most recent developments of the CBF

FIT2D V8.0: The Graphical User Interface

A.P.Hammersley

ESRF, BP 220, 38043 Grenoble Cedex, France

FIT2D is used at the ESRF and at a number of other institutes for a wide variety of data analysis purposes, including detector distortion correction, 2-D powder data integration, and small and wide angle scattering. During the last year a free portable graphics system has been developed (presently X-11 and PostScript output is available).

The main user interface has been a keyboard menu, but presently a "Graphical User Interface" (GUI) is under test at the ESRF. This interface aims to provide the most used functionality for different scientific specialities collected together under self-contained graphical menus. A file selection tool allows easy choice of input and output files, and "HELP" buttons provide detailed information on the various menus and options.

The "Powder Diffraction" interface presently provides a number of options which are of wider use. Arbitrary regions of data may be graphically defined and integrated to 1-D or 2-D azimuth/2-theta regions. *e.g.* This option allows the 1-D profile around the azimuth or radially to be integrated for further analysis.

FIT2D is available by ftp for most common workstations.

An Investigation of Crystallisation Kinetics in Oriented PET Random Copolymer Films Using 2D SAXS Correlation Function Analysis.

E.L.Heeley¹, D.J.Hughes¹, A.Mahendrasingam¹, D.MacKerron² and W.Fuller¹

¹ Department of Physics, University of Keele, Staffordshire, ST5 5BG, U.K.

² ICI Films R&T, Materials Research Centre, Wilton, Middlesborough, Cleveland, TS6 8JE, U.K.

The supermolecular structure of several oriented annealed films of poly(ethylene terephthalate) (PET) based random copolymers are investigated by small- and wide-angle X-ray scattering (SAXS, WAXS), in addition to physical density measurements.

The 2-D SAXS patterns are analysed by the use of 1D correlation functions, which reveal detailed information about the lamella morphology of the film involved. Determination of the amount of induced crystallisation in the film sample using X-ray and physical techniques, enables comparisons to be made between the various copolymers and the homopolymer PET films.

Initial conclusions can be drawn from these results, indicating that the presence of just a few percent of a certain copolymer in a PET film, will affect its crystallisation kinetics when compared with the homopolymer film under the same processing conditions.

Rapid 2-D SAXS/WAXS Measurements During the Deformation of Synthetic Polymers.

D.J.Hughes¹, A.Mahendrasingam¹, E.L.Heeley¹, C.Martin¹, W.B.Oatway¹, E.Towns-Andrews², M.E.Vickers³ and W.Fuller¹.

¹ Department of Physics, Keele University, Staffordshire, ST5 5BG, UK.

² CCLRC Daresbury Laboratory, Warrington, WA4 4AD, UK.

³ Department of Materials Science and Metallurgy, University of Cambridge, Cambridge, CB2 3QZ, UK.

In recent years there has been a trend towards the simultaneous collection of SAXS and WAXS data. Various strategies have been adopted in order to collect both SAXS and WAXS simultaneously. However, the only solution that provides adequate

time-resolution for the in-situ investigation of polymer deformation is to use two electronic detectors. In order to collect the full two-dimensional data from an oriented polymer it is essential that they are both area detectors.

An integrated system has been developed that is capable of uniaxially drawing a synthetic polymer at rates up to those typical in industrial processing and at temperatures from ambient to 350°C. In order to collect X-ray diffraction data we have commissioned a flexible detector system that is based around Photonic Science CCD based area detectors. These detectors operate at a frame rate of 25s⁻¹ therefore giving a minimum temporal resolution of 40ms. The system uses a powerful Synoptics i860 video frame-grabber which is capable of simultaneously digitizing and storing up to three synchronized video signals.

It has been possible to use this detector system for the collection of rapid 2-D simultaneous SAXS/WAXS data during the deformation of various industrially relevant synthetic polymers including PE and PET. A further development of the system has enabled the simultaneous load/extension data to be collected during an experiment, which is highly useful to correlate macroscopic yielding with changes observed in the X-ray scattering. Results of these studies will be presented. Other examples of the use of the system will also be given including high spatial resolution and high temporal resolution studies.

Collagen Fibril Orientations in Tissues and their Relationship to Mechanical Properties

D.W.L.Hukins

University of Aberdeen

Collagen fibrils provide tensile reinforcement in connective tissues. The efficiency of reinforcement is defined by an orientation distribution function. This function then relates tissue structures to their mechanical properties. A single X-ray diffraction pattern provides the orientation distribution function for the tissue site from which it was recorded. The method of calculating orientation distribution functions, the application to a variety of connective tissues, the application of the results and future developments will be described.

The "RAPID" X-Ray High Rate Detector System

A.Jones, W.Helsby, R.Lewis and C.Hall

CCLRC Daresbury Laboratory, Daresbury, Warrington, WA4 4AD

Multiwire Proportional counters (MWPCs) have been regularly used for small angle scattering experiments on the SRS. They have excellent time resolving properties, good efficiency, large area and dynamic range limited only by the memory size. However, they have local and global count rate limitations, in particular the global count rate is limited to 1 million photons per second.

The 'RAPID' X-ray detector system developed by the Daresbury Detector Group will provide at least a tenfold improvement in the local and global count rate performance over present systems. The poster will describe the system and present some results obtained during beamline commissioning.

A High Temperature Shear Flow Study of Pluronic P-85 in Aqueous Solution

S.M.King¹, V.M.Cloke², H.E.Hermes (nee James)², R.Done³, T.Cooper⁴, and C.Washington⁵

1 ISIS Large-Scale Structures Group, CCLRC

2 Department of Chemical Engineering, Imperial College, London

3 ISIS Project Engineering Group, CCLRC

4 ISIS Sample Environment Group, CCLRC

5 Department of Pharmaceutical Sciences, University of Nottingham

The commercially produced Pluronic (also variously known as the Synperonic, Poloxamer and Proxanol) series of water-soluble oxyethylene-oxypropylene block copolymers are amongst the most widely used non-ionic emulsifiers in the pharmaceutical, cosmetics and food industries. Above about 15°C the oxyethylene blocks are more soluble in water than the oxypropylene blocks. This results in the formation of copolymer micelles and a rich variety of phase behaviour.

In this work we have been studying the structure of micelles of Pluronic P-85, which has the approximate composition $\text{HO}-(\text{C}_2\text{H}_4\text{O})_{26}-(\text{C}_3\text{H}_6\text{O})_{39}-(\text{C}_2\text{H}_4\text{O})_{26}-\text{H}$, in a dilute, flowing, solution at elevated temperatures (25 - 80°C) - conditions not dissimilar to those that may be encountered during product processing - using a new Poiseuille Shear Flow apparatus. This apparatus allows us to mimic pipeline flow conditions in-situ on the SANS beam

line ("LOQ") at ISIS.

It is found that as the temperature of the solution is raised the SANS pattern changes dramatically. In particular, Brown & co-workers (principally using light scattering) have shown that around 65°C there is a transition from a spherical to a (flexible) rod-like micellar geometry. We are able to align these rod-like micelles in the shear flow field, thereby enabling a more detailed examination of the changes taking place to be made.

By fitting the data to various models for the scattering it has been possible to construct a picture of the changes in both shape and size that take place in the solution as it is heated. We find that around room temperature the scattering approximates very well to that from individual polymer molecules or loose aggregates of copolymer molecules. Above about 30°C a more spherical geometry is adopted. The micelles then slowly become more ellipsoidal with increasing temperature. At around 50°C they have an axial ratio of about 2:1. Above about 60°C the micelles are becoming much more rod-like. Above 72°C the axial ratio exceeds 12:1. There is also some evidence that close to the "cloud point" of the solution the rod length decreases again.

Getting the Best from Detectors. Recent Progress.

R.A.Lewis

Daresbury Laboratory, Keckwick Lane, Warrington WA4 4AD.

State of the art detectors for non-crystalline diffraction are necessarily complex pieces of equipment. It has recently become clear that few users are able to obtain the optimum performance from the current detectors that are available on the SRS for non-crystalline diffraction. The talk will review some of the reasons for this, including common misconceptions about detector performance, detector artifacts and how to correct them and the implications for data quality. Work currently in progress by the detector group to eliminate some of the problems and make the systems more user friendly will be described.

In addition to improvements in the performance and usage of existing devices, a new detector system is nearing completion. The MicroGap detector RAPID system will provide a counting rate increase of more

than 20 times over the current best and represents a major step forward in the provision of quantum limited detector operation for synchrotron radiation diffraction experiments. Results from a highly successful recent beam test on station 16.1 will be shown and the project progress reported.

X-Ray Diffraction and Mechanical Studies of Oriented Fibres of Purified Titin

Q.Li¹, A.Vazina², K.W.Ranatunga³, D.Alexeev⁴, A.Soterious¹ and J.A.Trinick¹

1 Division of Molecular and Cell Biology, Veterinary School, University of Bristol.

2 Institute of Biological Physics, Puschino, Moscow.

3 Department of Physiology, Medical School, University of Bristol.

4 Department of Biochemistry, Edinburgh University.

Titin is a muscle-specific giant protein found in the sarcomere. Single titin molecules are about one micron long and span between the M- and Z-lines. The I-band portion of the molecule is thought to function as a molecular spring connecting the end of the thick filament to the Z-line. This spring develops tension when a muscle fibre is stretched. Its function is to transmit passive tension in the sarcomere and also keep the A-band central between adjacent Z-lines. The A-band region of the molecule is also thought to be elastic when not attached to the thick filament. The molecular mechanism of titin elasticity is not known.

We have studied the elastic properties of oriented fibres of titin molecules using X-ray diffraction and mechanical techniques. Fibres were prepared from rabbit titin made from skeletal and cardiac muscles. High resolution X-ray diffraction patterns were obtained from single titin fibres of 50-100 microns in diameter. These patterns are the first to be obtained from ordered titin fibres and they exhibit many discrete reflections. The reflections are indicative of β -structure and show that the titin molecules are aligned parallel to the fibre axis.

Mechanical measurements on the fibres were also performed. The steady state stress-strain curves show elastic behaviour similar to that of rubber. Neither the pH (5.5-8.0) nor ionic strength (50 - 200 mM) of the buffer significantly affects the development of steady-state tension. We have also measured the dynamic properties of the titin fibres by a small, fast (0.5 ms time scale) length perturbation. We found

that the dynamic stiffness first increased rapidly when the strain was increased from 0 to 50%, and then increased very slowly at higher strain levels. Both pH and ionic strength affect the dynamic stiffness. The stiffness values were larger when the pH and ionic strength values were low.

Ageing and Glycation of Ocular Tissue

N.Malik and K.Meek

Biophysics Group, Open University Oxford Research Unit, Berkeley Road, Boars Hill, Oxford, OX1 5HR, UK

Using stations 2.1, 7.2 and 8.2, the structural changes within eye tissues, such as the human cornea, sclera, lens and optic nerve, have been studied. The intermolecular spacing of corneal and scleral stromal type I collagen has been observed to increase with the age of the tissue. Changes in the low angle X-ray Bragg spacing have been observed as an effect of age in human lenses, and as an effect of cataract formation in both human and bovine lenses. Since sugar is known to attack long-lived proteins (a non-enzymic process known as glycation), the effects of various sugars have been studied in human cornea. The results suggest that certain sugars produce greater magnitudes of intermolecular change in collagen than do others. The glycation of corneal and scleral tissue was measured and found to increase with tissue age. A consequence of this non-enzymic reaction is the production of various fluorophores some of which are believed to possess cross-linking properties. Indeed, collagen-associated fluorescence was found to increase with tissue age such that there was a positive correlation between corneal/scleral age, collagen fluorescence and increases in collagen intermolecular spacing. The same sugar reaction is known to occur in lens and can produce cataract. This has been studied in the form of cold- and sugar-cataract. Age-related changes have also been observed in young and old human lenses. The effects of sugar bovine optic nerve have also been studied in a preliminary manner. They suggest that the changes in diffraction pattern observed at low angle, arise from alterations in collagen. The effect of various substances believed to prevent sugar-induced protein changes (*e.g.* aspirin) have also been observed both in the presence and absence of sugar.

Macromolecular Modelling Of Resting and Contracting Muscles Using X-Ray Diffraction Of Whole Muscles.

C.V.Miles¹, A.Svensson¹, J.Gandy², J.Bordas², R.Denny³⁺⁴, G.P.Diakun³, F.G.Diaz⁵, G.R.Mant³ and E.Towns-Andrews³.

1 Department of Physics and Astronomy, Leicester University

2 Department of Physics, Liverpool University

3 CCLRC Daresbury Laboratory, Warrington, WA4 4AD

4 Imperial College, London University

5 Departamento de Quimica Fisica, Universidad de Murcia, Spain

We are currently investigating the macromolecular structure of skeletal muscle fibres by building three-dimensional computer models of the myosin and actin filaments, and calculating the resulting diffraction patterns to compare with experimental X-ray data. Two-dimensional diffraction patterns calculated from the models are compared with high resolution patterns obtained by X-ray diffraction experiments on live frog sartorius muscles at rest and during isometric contraction, carried out on stations 2.1 and 16.1 of the SRS, Daresbury Laboratory. We present here our recent models for the rest and isometric contraction states and their implications for the actin-myosin interaction.

The main reflections of the rest pattern have been reproduced both in relative intensity and position. The broad axial width of the actin layer lines was attained by introducing a small random cumulative twist to the actin helix, which preferentially smears out the lower order layer lines. The myosin heads are arranged in a three-start helix with a true repeat of 42.9nm, whilst a regular displacement from the exact helical axial rise of 14.3nm has been introduced to account for the appearance of forbidden meridional reflections. Good agreement with the experimental data is achieved when the myosin heads are inclined at an angle to the filament backbone, and are slewed to wrap around it.

The change in the 3rd and 6th order meridional diffraction intensities observed during isometric contraction is reproduced by increasing disorder in the axial subunit positions. This also results in the loss of the regular helical distortions, and thus the removal of the forbidden reflections. The loss of Bragg lattice peaks along the layer lines has been reproduced by allowing the heads to take random slew angles about the filament backbone. Modelling

of various actin-myosin interactions show that this randomising does indeed take place if the crossbridges attach to the nearest actin monomer, thereby achieving the shortest possible bond lengths. This change of slew angle also goes some way to increasing the radius of the centre of mass of the heads, which is responsible for the observed intensity reversal of the equatorial reflections from rest to isometric contraction.

Characterising Disorder in Polycrystalline Fibres

R.P.Millane and W.J.Stroud

Whistler Center for Carbohydrate Research and Computational Science and Engineering Program, Purdue University, West Lafayette, Indiana 47907-1160 U.S.A.

Diffraction patterns from oriented polycrystalline fibres of some biopolymers show sharp Bragg reflections at low resolution that give way to continuous layer line intensities at high resolution. These kinds of patterns indicate disordering of the molecules within the crystalline domains of the fibres. Structure determination using data from such patterns has generally involved separating the data into Bragg and continuous components, and analyzing these in terms of crystalline and non-crystalline packing, respectively. This kind of analysis is only approximate, at best. Diagnosing the disorder and quantitatively accounting for its effects on diffraction are essential for accurate structure determination using data measured from these patterns.

We have developed two statistical models of disorder in fibres, along with expressions for the cylindrically averaged diffracted intensity [1,2,3]. The first model [1] is formulated in reciprocal space and can be used to calculate diffraction from fibres in which the lattice disorder is uncorrelated. The second model [2,3] is formulated in real space, is more flexible, and can be used to calculate diffracted intensities for the case of correlated lattice disorder.

To demonstrate the utility and applicability of these models, we have used them to quantitatively analyze the disorder in two polynucleotide fibres. The disorder in each fibre was diagnosed by matching features of diffraction patterns calculated from models to key features of the observed diffraction patterns. For both fibres, calculations using the model of uncorrelated disorder explains many

features of the diffraction patterns [4]. However, the diffraction pattern from one specimen showed evidence of correlated lattice disorder. Calculations incorporating correlated lattice disorder in the model significantly improved the match between the calculated and observed reflection profiles and the continuous intensity distribution on this pattern [3].

References

- [1] Stroud and R.P. Millane, *Acta Cryst.* **A51**, 771-790 (1995).
- [2] Stroud and R.P. Millane, *Proc. Roy. Soc. Lond. ser. A*, **452**, 151-173 (1996).
- [3] Stroud and R.P. Millane, *Acta Cryst.*, in press (1996).
- [4] Stroud and R.P. Millane, *Acta Cryst.* **A51**, 790-880 (1995).

MESA - A Programming Environment for the Study of Disordered Polymers

G.R.Mitchell, B.Rosi-Schwartz and Y-S.Chiou

Department of Physics, University of Reading

Disordered polymers, such as polymer melts, glasses and rubbers present a considerable challenge in terms of unravelling their local structure. Such materials are of tremendous technological importance and yet we know little of their local segmental interactions. This is especially important in relationship to miscible blends, polymer deformation and other bulk properties such as diffusion. Although X-ray and neutron scattering techniques provide plenty of data it has been unclear how to proceed in the analysis of these data. Scattering data obtained at synchrotron or neutron sources usually cover a broad Q-range. We have developed computational procedures which allow us to exploit the high data content in these broad Q-range data sets to provide detailed atomistic models of disordered polymers. These procedures have been incorporated within a new package: MESA (Molecular Editor for Structural Analysis). This poster describes the procedures and their application to particular structural problems. These procedures will be available for use via the WWW later in 1996.

A SAXS/WAXS Study on Silicalite Crystallization From a Clear Solution

P.P.E.A. de Moor, T.P.M.Beelen, R.A.van Santen

Laboratory of Inorganic Chemistry and Catalysis, Eindhoven University of Technology, The Netherlands.

The routes by which crystalline zeolites are produced from an amorphous gel or from a solution are complex, self-assembly processes involving numerous simultaneous and interdependent equilibria and condensation steps. Therefore the systematic study of the processes during the synthesis is complicated, especially because there are no indications for a universal mechanism [1]. A question of considerable debate is the nature of the synthesis gel and its role in the nucleation and crystal growth mechanisms. In the extreme case of a liquid-phase ion transportation mechanism [2], nucleation and crystal growth occur in the liquid phase. The gel phase present acts as a source of nutrients for the crystallization process. The other extreme is known as the solid hydrogel reconstruction mechanism [3]. Here nucleation and crystal growth occur in the heterogeneous gel or at the gel surface by a reconstruction or aging mechanism.

For the synthesis of silicalite we found considerable support for the hydrogel reconstruction mechanism [4]. Even in the crystallization of silicalite from a clear solution, gel particles were found to be present before crystallization [5]. Here we report the influence of the Si/Template and Si/OH ratios in the synthesis mixture on the formation of aggregates and the transformations therein. The Si/OH ratio appeared to be the key parameter in the formation of aggregates during the synthesis. Below a certain threshold value it was even possible to crystallize silicalite without the presence of aggregates in the solution. This points to a solution mediated crystallization.

References

- [1] Burkett, M.E. Davis, *Chem. Mater.*, 1995, **7**, 920-928
- [2] Gabelica, J.B. Nagy, G. Debras, E.G. Derouane, In: Proceedings of the sixth international zeolite conference, D. Olso, A. Bisio (Eds.), 914-924
- [3] Chang, A.T. Bell, *Catalysis Letters*, **8**, 1991, 305-316
- [4] Dokter, T.P.M. Beelen, H.F. van Garderen, C.P.J. Rummens, R.A. van Santen, J.D.F. Ramsay, *Colloids and Surfaces A: Physicochemical and Engineering Aspects*, **85**, 89-95
- [5] Dokter, H.F. van Garderen, T.P.M. Beelen, R.A. van Santen, W. Bras, *Angew. Chem. Int. Ed.*

Investigation of the Deformation of Polyethylene by Time-Resolved Simultaneous SAXS/WAXS and Stress/Strain Measurements.

W.B.Oatway, D.J.Hughes, A.Mahendrasingam, E.L.Heely and W.Fuller

Department of Physics, Keele University, Keele, Staffordshire, ST5 5BG, UK

A polymer camera system has been developed at Keele University which allows the collection of simultaneous time-resolved small- and wide- angle X-ray scattering (SAXS and WAXS) and stress/strain data during the uniaxial deformation of a sample. WAXS data are recorded using a Photonic Science charge-coupled-device (CCD) based area detector. SAXS data are collected using a gas-filled multiwire area detector. Strain data are measured directly from lines marked on the sample, as viewed from video images recorded during the experiment. The tensile force, as experienced by the sample during the draw, is measured using a bridge circuit type strain gauge.

An example of the use of this system is illustrated by the drawing of a medium density polyethylene at a rate of 100%/min with sample environment temperatures of 70°C and 110°C. It is shown how the observed diffraction data can be related to specific

Neutron Diffraction Study of B-DNA Hydration

L.H.Pope¹, M.W.Shotton¹, V.T.Forsyth¹, P.Langan², H.Grimm³, A.Ruprecht⁴, R.Denny⁵ and W.Fuller¹

1 Physics Department, Keele University, Staffordshire, ST5 5BG, U.K.

2 ILL, Grenoble, France

3 Insitute fur Festkorperforschung, Julich, GMBH

4 Arrhenius Laboratory, Stockholm University, Sweden

5 CCLRC Daresbury Laboratory, Daresbury, Warrington, U.K.

A high angle neutron diffraction study of the distribution of water around the B conformation has been carried out using the diffractometer D19 at the ILL, Grenoble. Datasets were recorded for DNA in both a H₂O and a D₂O environment. Various data analysis techniques involving CCP13 software have been exploited to generate Fourier maps in which the peaks correspond to the water distribution around the DNA conformation. An ordered water network has been observed in both the major and minor groove. Refinement of these water positions is currently being carried out from which a more detailed picture of the hydration will be revealed.

Structural Modelling of Nylons with Two Hydrogen Bond Directions

J.Puiggali, J.E.Aceituno, L.Franco, E.Navarro and J.A.Subirana

Department d'Enginyeria Quimica, ETS d'Enginyers Industrials, Universitat Politecnica de Catalunya, Diagonal 647, Barcelona 08028, Spain

Nylons can be synthesized by the condensation of amino acids (nylons n) or diamine and dibasic acids (nylons m,n). In spite of the differences in the disposition of amide groups and in the methylene content of the repeat units, only two basic structures have been reported at low temperature. The first one is the so called a-form [1] characteristic of nylon 66 and many other polyamides, which are organized as parallel sheets of hydrogen bonded molecules with an extended conformation. The second structure, the g-form [2], corresponds to a pseudo-hexagonal form which is also organized in parallel sheets of hydrogen bonded molecules.

We have recently synthesized and characterized several n,3 and n,5 polyamides. The X-ray diffraction and electron microscopy results obtained, taken together with work carried out on low molecular weight model compounds studied by X-ray crystallography [3,4] and quantum mechanical calculations [4], indicate a different structure for these polymers [5-7] than the conventional forms of nylons. Thus, they are organized as a network of hydrogen bonded molecules with two different hydrogen bond orientations which form an angle of about 60° or 120° amongst them. Moreover the X-ray fibre diffraction patterns and electron microscopy results have shown that n,3 and n,5 polyamides crystallize in different systems which depend on the value of n.

The linked-atom least-squares (LALS) method has been used to build and refine suitable models. Electron and X-ray diffraction patterns have also been simulated with the CERIUUS program (Molecular Simulation Inc.). In some cases stereochemically satisfactory models have been subject to an analysis of the energy, using the AM1 and PM3 semi-empirical methods. The refined models show that although two hydrogen bond directions are characteristic of both n,3 and n,5 nylons, there is an essential difference: in the malonamide derivatives the two carbonyl groups are mutually oriented at about 120°, whereas in the

glutaramide derivatives the two carbonyl groups are oriented at about 60°.

References

- [1] Bunn, C.W.; Garner, E.V. *Proc. R. Soc. London Ser. A.* 1947, **189**, 39.
- [2] Konoshita, Y. *Makromol. Chem.* 1959, **33**, 1.
- [3] Navarro, E.; Puiggali, J.; Subirana, J.A. *Makromol. Chem. Phys.* 1995, **196**, 2361.
- [4] Navarro, E.; Aleman, C.; Puiggali, J. *J. Am. Chem. Soc.* 1995, **117**, 7307.
- [5] Aceituno, J.E.; Tereshko, V.; Lotz, B.; Subirana, J.A. *Macromolecules* 1996, **29**, 0
- [6] Navarro, E.; Franco, L.; Subirana, J.A.; Puiggali, J. *Macromolecules* 1995, **28**, 8742.
- [7] Navarro, E.; Aleman, C.; Subirana, J.A.; Puiggali, J. *Macromolecules* 1996, **29**, 0.

Chain Conformations in Polyurethanes: A SAXS & SANS Study

A.J.Ryan^{1,2}, S.N.Naylor¹, N.J.Terrill¹ and S.King³

1 UMIST Materials Science

2 CCLRC Daresbury Laboratory

3 CCLRC Rutherford Appleton Laboratory

Segmented polyurethanes are statistical block copolymers comprising incompatible hard and soft blocks. A range of poly(ether-urethane) copolymers has been synthesised in order to verify which is the primary driving force behind microphase separation: block incompatibility or crystallisation of the segments. Two classes of copolymer have been synthesised: one class contained a semi-crystalline 4,4'-methylene diphenyl diisocyanate (4,4'-MDI) and butanediol (BDO) based hard segment, the other contained an amorphous hard segment based on a blend of 2,4- and 4,4'-methylene diphenyl diisocyanate (2,4/4,4'-MDI) and BDO. The soft segment in both types of copolymer was polypropylene oxide (PPO). The materials were synthesised with various hard segment contents: 25, 50 and 75% by weight. The PPO samples had molecular weights that ranged from 400 to 4000.

Characterisation of the materials involved heating the materials until homogeneous in order to remove all traces of prior thermal history, and then annealing the samples at different temperatures. Quenching in liquid nitrogen was used to "freeze-in" the resultant morphologies. These samples were then analysed using separate differential thermal analysis experiments (DTA) and X-ray scattering

experiments. Both the 4,4'-MDI and 2,4/4,4'-MDI copolymers which contained low hard segment contents or low molecular weight soft segments were shown to be homogeneous after annealing. Annealing had little effect on these materials. However, annealing the higher molecular weight 4,4'-MDI copolymers promoted crystallisation and produced larger microdomains with sharper interfaces. As a consequence of this, the PPO chains were stretched more in the 4,4'-MDI copolymers than in the 2,4/4,4'-MDI materials. In contrast, annealing had little effect on the 2,4/4,4'-MDI copolymers, evidence that crystallisation plays an important part in the microphase separation process.

The kinetics of microphase separation and crystallisation were investigated using time-resolved X-ray scattering experiments. Several models were used, including Avrami and time-dependent Ginzburg-Landau (TDGL) analysis. Aspects of the microphase separation process fitted both the spinodal decomposition (SD), and nucleation and growth (NG) models. However, the latter was favoured because the Avrami equation was seen to be in excellent agreement with that of the data, and fit the data better than the SD models. The thermal history of the 4,4'-MDI materials was observed to have an important effect on the melting behaviour of the samples, possible causes being chain branching and side-reactions.

Changes in the conformation of the PPO soft segment were investigated using small-angle neutron scattering (SANS). A phase contrast matched copolymer was used to measure changes in the radius of gyration of the soft segment with temperature in a semi-crystalline, microphase-separated material. The Debye model fit the data well, and showed the soft segments to initially be in somewhat extended conformations, as a result of chain stretching brought on by movement of the hard segments during microphase separation/crystallisation. On heating, some disordering occurred as the soft segments began to pull hard segments out of the domains, to take the form of random coils. In addition, SANS patterns from hydrogenous polymers showed excellent agreement with SAXS patterns, confirming that the microdomains present in the microphase separated materials were the scattering entities in both techniques, and provided confidence in the spatial information so obtained.

Changes in the long period, obtained using

correlation function analysis on SAXS data for a hydrogenous copolymer, correlated well with changes in the SANS data obtained for the contrast matched equivalent. The sample was shown to begin to disorder on softening at $\sim 100^\circ\text{C}$ and was mostly phase mixed by 180°C with some isolated crystalline domains present. At $\sim 200^\circ\text{C}$ these larger domains melted as the material became homogeneous.

The experimental studies confirmed the domination of crystallisation over microphase separation due to its greater enthalpic driving force.

A High Angle Neutron Fibre Diffraction Study of the Distribution of Water Around the B Conformation of DNA.

M.W.Shotton¹, L.H.Pope¹, V.T.Forsyth¹, P.Langan², H.Grimm³, A.Rupprecht⁴, R.Denny⁵ and W.Fuller¹

1 Physics Department, Keele University, Staffordshire ST5 5BG.

2 ILL Grenoble, France.

3 Institute für Festkörperforschung, Jülich, GmbH.

4 Arrhenius Laboratory, Stockholm University, Sweden.

5 Imperial College / Daresbury Laboratory.

A high-angle neutron fibre diffraction study of the distribution of water around the B-form DNA has been carried out using the D19 diffractometer at the Institut Laue-Langevin, Grenoble. This instrument was used in fibre precession geometry to facilitate the efficient coverage of a large area of reciprocal space. The sample was prepared using the wet spinning method of A.Rupprecht of Stockholm University. This method produced a sample of excellent crystallinity and orientation.

Data were recorded with the sample hydrated firstly with H_2O and then with D_2O . The exchange of H_2O by D_2O around the DNA resulted in significant differences in the recorded diffraction pattern. Furthermore the exchange enabled the use of Fourier Synthesis techniques in the identification of ordered water around the DNA.

There appears to be a regular distribution of water in both the minor and major grooves, with both distributions exhibiting the ten-fold helical symmetry characteristic of B-DNA. A least squares refinement of the water positions and occupancies is now being conducted, and the results will be discussed at the workshop.

SAXS/WAXS/Raman Investigations into Phthalocyanines.

A.D.Stennett¹, H.F.Gleeson¹, G.K.Bryant¹, N.B.McKeown², A.J.Ryan³ and W.Bras⁴

1 Dept. of Physics and Astronomy, University of Manchester, M13 9PL.

2 Dept. of Chemistry, University of Manchester, M13 9PL.

3 Dept. of Material Sciences, UMIST.

4 AMOLF, Netherlands.

Some substituted phthalocyanines (Pcs) are of interest due to their optical properties and medical applications. The type of mesophases that can be formed are lyotropic and thermotropic and depend greatly on the type and number of substituents on the edge of the molecule.

We present results from an investigation into three substituted phthalocyanines known to show lyotropic and/or thermotropic liquid crystal phases. The physical properties of these compounds are determined using simultaneous SAXS, WAXS and Raman spectroscopy.

Preliminary investigations have indicated columnar nematic, hexagonal columnar and crystal hexagonal columnar phases with interdisc spacings of about 3.3\AA and intercolumn spacings of 16\AA , 22\AA & 25\AA . Simultaneous Raman spectroscopy has shown features changing with these phase transitions.

In one of the samples, an Ia3d structure has been seen which, for calamitic lyotropic molecules might indicate a bicontinuous cubic structure. A discotic structure like this would be highly stressed due to the deformations required at the intersections of the columns. The size of the unit cell for this structure is about 80\AA , only 3 to 4 times the diameter of the molecule itself.

Crystallisation and Texture Development During the Processing of Polymer Films

N.J.Terrill¹, E.Towns-Andrews², J.P.A.Fairclough¹, B.U.Komanschek², A.J.Ryan¹ and R.J.Young¹

1 Manchester Materials Science Centre, UMIST, Grosvenor Street, Manchester, M1 7HS, UK

2 CCLRC Daresbury Laboratory, Warrington, WA4 4AD

More than three-quarters of the polymers used in the world are semicrystalline. Their processing relies on the shaping of molten polymers in moulds or by dies

and the stabilisation of that shape by crystallisation [1]. The growth of polymer crystals is well understood and there are reliable theories to predict kinetics; the understanding of the nucleation process is, however, less satisfactory.

The available theories are over-complicated and somewhat unphysical [2]. There is good reason why this should be the case; access to the nucleation step is experimentally difficult whereas studies of crystal growth are easy enough to be used in undergraduate laboratory classes [3]. In order to separate nucleation from growth, two types of experiments have been performed on homo-polypropylene.

Slow crystallisations with long induction times were studied by simultaneous small- and wide-angle X-ray scattering. This showed clear development of small angle scattering, due to density fluctuations, with a characteristic length scale of 200Å, prior to the presence of crystals identified by wide-angle scattering [4].

The initial growth of structure followed the kinetics of spinodal decomposition. Once wide-angle diffraction from crystals (atomic order on the 1Å scale) was observed, the kinetics reverted to those of nucleation and growth. Rapid crystallisations were studied by melt extrusion of a tape. The extrusion of tape is a steady-state process where the distance down the spin-line is directly proportional to the crystallisation time.

This allowed long data collection times (minutes) for very short crystallisation times (milli-seconds). Prior to the development of crystallinity, well resolved, oriented small-angle patterns could be collected with length scales (50-300Å) and intensities that grew down the spin-line. These early patterns had the shape associated with spinodal decomposition.

Once crystallisation was observed in the wide-angle region the shape of the small-angle pattern changed from that characteristic of sinusoidal density fluctuations to that characteristic of lamellar crystals. These two experiments confirm that spinodal decomposition of chain segments with different average conformations is the nucleation step in polymer crystallisation.

References

[1] "Plastics Engineering", R.J. Crawford, Pergamon Press, Oxford.

- [2] J.I. Lauritzen and J.D. Hoffman, *J.Res.Natl.Bur.Stand.Sect.A*, 1960, **64**, 73.
- [3] J.D. Hoffman, J.I. Lauritzen, E.Passaglia, G.S. Ross, L.J. Frohler and J.J. Weeks, *Kolloid.Z.Poly.*, 1969, **231**, 564.
- [4] J.D. Hoffman, G.T. Davis and J.I. Lauritzen, in "Treatise on Solid State Chemistry", Plenum, New York, 1976.
- [5] D.M. Sadler, *Polymer.Comm.*, 1986, **27**, 140. D.M. Sadler, *Polymer*, 1987, **28**, 1440. "Introduction to Polymers", R.J. Young and P.A. Lovell, Chapman and Hall, London. Imai, K. Kaji, T. Kanaya, Y. Sakai, *Phys.Rev B Condensed Matter*, 1995, **52**, 12696.

Tubular, Spherical and Layered Self-Assembly in Novel Thermotropic Systems

G.Ungar, V.S.K.Balagurusamy, J.P.Zhou and V.Percec

Department of Engineering Materials, University of Sheffield, Sheffield & Case Western Reserve University, Cleveland, Ohio

Thermotropic compounds containing unorthodox mesogens are investigated by X-ray diffraction. Rather than being rod-like or disk-like, these mesogens are fan-shaped, cone-shaped or fully flexible. They assemble into spherical, tubular or layered aggregates, forming cubic, columnar or smectic liquid crystal phases. Examples of structure determination of these phases are presented using low-resolution crystallography, with electron density reconstructions. Isomorphous replacement is used in 1- and 2-dimensional cases. The structure of a new thermotropic cubic phase is presented.

Diffraction from Fibres of Filamentous Bacteriophage using Soft X-rays

L.C.Welsh¹, M.F.Symmons², C.Mitsch¹, E.A.Marseglia¹, C.Nave³, R.N.Perham², D.A.Marvin², S.Stuhrmann⁴, C.Trane⁴ & H.B.Stuhrmann⁴.

1 Cavendish Laboratory, University of Cambridge, Cambridge CB3 0HE, UK.

2 Department of Biochemistry, University of Cambridge, Cambridge CB2 1QW, UK.

3 CCLRC Daresbury Laboratory, Warrington, WA4 4AD, UK.

4 Makromolekulare Strukturforchung im Institut Fur Werkstofforschung, GKSS, Postfach 1160, D-21494 Geesthacht, Germany.

The filamentous bacteriophage (Inovirus) virion is about 6 nm in diameter and 1000 to 2000 nm long,

comprising a helical tube of major coat protein subunits surrounding a core of single-stranded circular DNA. We have used fibre diffraction to develop models for the protein coat of various strains [1-2]. The analysis of the DNA structure has proven more difficult because the DNA comprises at most 14% by weight of the virion; the DNA does not have the same helical symmetry as the protein coat. By measuring diffraction on each side of the phosphorus K-absorption edge, we hope to determine the radius of the phosphate groups, to aid in building models of the DNA in the virion.

Our preliminary measurements established that X-ray diffraction from oriented fibres of Inovirus at wavelengths near the phosphorus K-absorption edge was detectable. Sample and air absorption is very severe at X-ray wavelengths near the phosphorus K-edge, so experiments must be conducted in a vacuum [3], and the fibres must be very thin and isolated from the vacuum. We experimented with various sample geometries to optimise the diffraction signal from the fibres, and found one that was effective.

Three strains of Inovirus were examined: Pf1, Pf3, and the Y21M mutant of fd. The best data were obtained from the fd and Pf1 strains. Clear intensity changes as the wavelength was altered across the K-absorption edge were seen in diffraction patterns from the fd strain, which contains about twice as much DNA per protein as Pf1. The intensity change is observed in a region of the equatorial diffraction pattern (0.029 -1) known to have a substantial DNA contribution [4]. Obtaining accurate integrated intensities from the diffraction data has proven difficult because the data are rather noisy. Further diffraction experiments are planned to obtain improved data to resolve structural questions concerning DNA packaging in Inovirus.

References

- [1] Marvin, D.A., Hale, R.D., Nave, C. & Helmer Citterich, M. (1994) *J. Mol. Biol.* **235**, 260-286.
- [2] Gonzalez, A., Nave, C. & Marvin, D.A. (1995) *Acta Cryst.* **D51**, 792-804.
- [3] Stuhrmann, S., Htsch, M., Trame, C., Thomas, J. & Stuhrmann, H.B. (1995) *J. Synchrotron Rad.* **2**, 83-86.
- [4] Symmons, M.F., Welsh, L.C., Nave, C., Marvin, D.A. & Perham, R.N. (1995) *J. Mol. Biol.* **245**, 86-91

Modelling Diffraction from Poly(ethylene terephthalate)/Poly(ethylene naphthalene-2,6-dicarboxylate) (PET/PEN) Crystalline Random Copolymers

G.E. Welsh and A.H. Windle

Department of Materials Science and Metallurgy University of Cambridge Pembroke Street CB2 3QZ

PET/PEN random copolymers of all compositions are able to crystallize under conditions of hot drawing, with marked enhancement of crystallinity on subsequent annealing. Since random copolymers containing 50mol% PET are the most extreme case, this composition has been used in computer modelling to investigate the crystalline structure of these random copolymers.

The main features of fibre diffraction patterns from samples containing 50mol% PET may be summarised as follows. The layer lines are non periodic and their spacing shows that crystallites in the sample consist of polymer chains with equal numbers of PET and PEN monomers arranged randomly in the chain direction. The Equator, first, fourth, fifth and sixth layer lines have distinct Bragg peaks. The second and third layer lines are weak unsampled lateral streaks.

The sampling of layer lines indicates that there must be some degree of register between the neighbouring random chains within the crystallites. We have used 2-D models in which monomers are represented by delta functions, to investigate how the extent of register between the chains affects the appearance of the diffraction patterns. Extending the models into three dimensions has shown that only relatively small amounts of movement between neighbouring chains are needed to produce crystallites whose diffraction patterns show all the main features of fibre diffraction patterns from 50mol% PET/PEN random copolymers.

Collagen Structure: Fibrils and Microfibrils

T.J.Wess¹, A.Hammersley², L.Wess¹, A.Miller¹,
D.Prockop³, P.Fratzl⁴ and D.Hulmes⁵

1 University of Stirling

2 ESRF

3 Thomas Jefferson University

4 University of Vienna

5 University of Edinburgh

Current modelling of collagen structure has been done on two levels.

1) The structure of the type I fibril was analysed in the light of fibril tip shape, accretion models and radial (or spirallar) distribution of collagen molecules in the fibril. The equatorial diffraction pattern of type I collagen from tendon was used to determine the relationship between disordered and ordered parts of the fibril. Previous models of fibril structure were also tested by construction of lateral sections through model fibrils, and the radially averaged intensity terms of a model diffraction pattern obtained.

The best fit to the experimental data was found by producing radial models where the accretion to the fibril surface was by addition of microfibrillar pentamers. After energy minimisation using a simple Lennard Jones potential, the fibril structure produced a satisfactory fit with the diffraction data. The transverse section of the model fibril contained grain boundaries between individual segments of crystallinity. A full explanation of the relationship between diffuse and Bragg peaks requires the modelling of a 1-D (67nm longitudinal) segment, with both the gap overlap and gap/overlap interface being used to produce a full structural simulation. The anisotropic interactions within microfibrils however are not considered in this structure.

2) The contention between sheet type structures and microfibrillar arrangements has also been investigated. Models of both types were constructed with a number of other parameters such as telopeptide conformation and molecular mobility considered. The Intensity terms of the Fourier transform from each representative structure was compared to the Bragg peak intensities of crystalline reflections obtained by the use of FIT2D to remove the diffuse equatorial component.

With a search of over 2×10^8 conformations, no sheet

structure produced a tenable fit with the data. No 2-D staggered microfibrils produced a suitable fit and only the 1-D microfibril group contained favourable structures. On analysis of the best fit with the data it was found to contain a telopeptide conformation that would support intermolecular crosslinks. This data therefore substantiates the microfibril as a building unit between molecule and fibrillar levels of organisation. The twisting path taken by individual molecules in the microfibril structure may provide the basis for the biomechanical observations of relative inextensibility in highly aligned fibril structures.

References

- [1] Hulmes, D.J.S. Wess, T.J. Prockop, D.J. Fratzl, P. (1995) "Radial packing order and disorder in collagen fibrils" *Biophys J.* **68** 1661-1670.
- [2] Wess, T.J. Hammersley, A.P. Wess, L. Miller, A. (1995) "TypI collagen packing, Conformation of the triclinic unit cell" *J.Mol.Biol.* **248** 487-493.

Advantages of Absolute Calibration in Small-Angle X-Ray and Neutron Scattering Studies of Polymers and Colloids

G.D.Wignall

Solid State Division, Oak Ridge, National Laboratory, Oak Ridge, Tennessee 37931-6393.

Absolute calibration forms a valuable diagnostic tool for the detection of artifacts, to which small-angle X-ray and neutron scattering (SAXS and SANS) techniques are particularly vulnerable. This lecture emphasises the importance of placing data on an absolute scale, in the form of a differential scattering cross section $d\Sigma/d\Theta(Q)$, per unit sample volume (in units of cm^{-1}). General methods that are available for absolute scaling of SAXS and SANS data are reviewed, along with estimates of the degree of consistency which may be achieved between various standards. In order to minimise the time associated with calibration procedures, emphasis is placed on developing pre-calibrated, strongly scattering standards which may be run in brief time periods (~ 1 minute). Special attention is paid to standards that can be used for either SAXS or SANS experiments, where each sample has been independently calibrated for both types of incident radiation. These calibrations have been tested by calculating the theoretical relationship between the X-ray and neutron cross-sections.

The use of absolute units is not essential for the measurement of spatial dimensions (*e.g.* domain sizes, radius of gyration of polymer molecules *etc.*). However, the cross-section varies as the sixth power of the dimensions and is a very sensitive indicator of whether an appropriate structural model has been chosen. Thus, scattering from colloidal micellar solutions may be modelled by core-shell structures as a function of a set of parameters such as the inner/outer radius, composition *etc.* On an arbitrary scale, it is possible to produce excellent fits of the shape of the scattering, which may be in error by orders of magnitude in intensity. Absolute calibration allows such artifacts to be recognised, and the model parameters may be restricted to those which reproduce the observed cross-section. Conversely, even an approximate ($\pm 25\%$) absolute calibration is sufficient to confirm the assumptions of the structural model chosen. Because the literature often contains general formulae, as opposed to practical examples of how such model calculations are actually accomplished, such comparisons will be illustrated via a range of examples on different polymeric and colloidal systems.

Data Collection, Processing and Analysis Techniques in Time-of-Flight Laue Diffraction

C.C.Wilson

ISIS Facility, CCLRC Rutherford Appleton Laboratory, Chilton, Didcot, Oxon OX11 0QX, UK

Single crystal data collected using the time-of-flight Laue diffraction technique at a pulsed neutron source should be viewed somewhat differently from that collected by more traditional, steady state, means. The nature of the method leads to large 3-D volumes of reciprocal space being accessed in a single measurement, with important implications for any experiment carried out using this method.

First, the 'Bragg' intensities in such an experiment are only part of the story; the method also accesses the regions between Bragg peaks, to examine for example diffuse scattering in an efficient and straightforward way.

Secondly, the data are collected at a variety of wavelengths, sorted using the time-of-flight method; the consequent data corrections are more complicated than in monochromatic methods.

Thirdly, the collection of data using a position-sensitive detector always calls for caution; it is vital to understand and appreciate what is happening with the detector and to develop ways of optimising data extraction taking this into account.

The rewards for correctly designed experiments, however, are rich. The Laue method offers a degree of flexibility in data collection which lends itself to the rapid collection of data sets (whether with X-rays or neutrons), making the technique ideal for the study of structural changes. Following structural trends as a function of external variables is a rapidly growing area in condensed matter science, and the Laue technique offers the best opportunity for single crystal work to join in this development. Increasingly also, the measurement of the total diffraction pattern, including the diffuse scattering, will become more important. The Bragg intensities give the average structure throughout the sample, the diffuse scattering can give information on local structure and hence complete the picture of molecular structure. The most quantitative results in this area are promised by neutron diffraction techniques.

This talk will address a range of issues concerning the optimal exploitation of the information available in a diffraction pattern collected by the time-of-flight Laue method. Topics covered will include: the general design of such an instrument; procedures for carrying out experiments; the extraction of the required data, including novel data collection methods and optimised intensity extraction software; the information contained in the non-Bragg scattering components of the pattern; and the development of methods for collecting, normalising and interpreting this scattering.

CCP13 Travelling Fellowships

CCP13 Travelling Fellowships (£500) are intended to supplement awards to younger UK researchers travelling abroad for a conference involving fibre diffraction in order to give them the opportunity to visit a few fibre diffraction laboratories in the host Country. The £500 is intended to cover the extra travel, accommodation and subsistence costs in the host country involved in visiting these laboratories. It is not intended to cover the basic cost of attending the main conference. The recipients will be asked to report on their visits in a talk to the May Annual Meeting of CCP13 and also to contribute a short (1 page) report for the annual "Fibre Diffraction Review". Current PhD students must have their application countersigned by their research supervisor if they wish it to be considered. Two awards will be made each year.

Application deadline for travel in Summer 1997: MARCH 31st, 1997

Application forms can be obtained from the CCP13 secretary, Dr. G. Mant (g.r.mant@dl.ac.uk).

If awarded, the scholarship will be sent by cheque, once the travel arrangements of the Fellow have been confirmed.

CCP13 Visiting Scientist Fellowship Programme

From time to time the CCP13 Committee will invite an outstanding scientist from overseas to take part in the May Annual CCP13/NCD Workshop and, before or after the Workshop, to visit various contributing laboratories in the UK over a period of one or two weeks to talk to and advise on fibre diffraction methods and results.

CCP13 members are welcome to put forward to the Committee the names and addresses of possible visitors, preferably with some details in writing, including suggestions about which UK scientists/laboratories should be visited.

The 6th Annual CCP13/NCD Workshop

“Diffraction from Fibres and Polymers”

7 - 8th May 1997

at

Daresbury Laboratory

For further details please contact The Conference Office, Daresbury Laboratory, Warrington, Cheshire, WA4 4AD. (Tel: 01925 603235. Fax: 01925 603195 Email: conference@dl.ac.uk WWW: <http://www.dl.ac.uk/SRS/CCP13/workshop97>)

Alpbach Workshop: 1997

A workshop dedicated to the description and comparison of the structures and interactions of the well-known and newly identified coiled-coil α -helical molecules, of different collagen types and of other fibrous biological materials:

COILED-COILS, COLLAGEN & CO-PROTEINS II

September 7 - 13, 1997

at

Boglerhof Hotel, Alpbach, Austria

The Workshop provides an opportunity for a formal tribute to be made to the outstanding achievements of Professor Carolyn Cohen.

Contact: Prof. J.Squire, Biophysics Section, Blackett Laboratory, Imperial College, London, SW7 2BZ, UK. / e-mail: j.squire@ic.ac.uk / fax: +44 (0) 171 589 0191

SIEMENS

Finally - an easy-to-use X-ray diffraction system for analyzing polymers

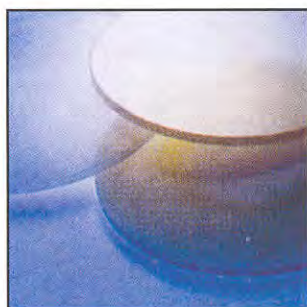
The Siemens Area Detector and GADDS (General Area Detector Diffraction System) polymer software are faster, more flexible and easier to run than any other X-ray diffraction system available today. Featuring pop-up menus and real-time color display as part of a graphics-oriented user interface, the only thing missing is competition.

- Ideal for texture analysis, percent crystallinity and other applications, including QC
- Easily measures d-spacing, angles and intensities from any pixel location
- Versatile data files can be used with powder diffraction software and for phase identification and profile fitting



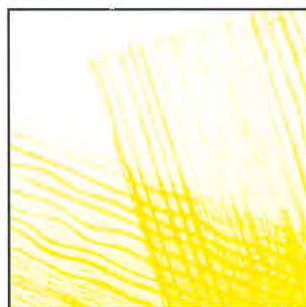
Plastics

True QC instrument for measuring intensities and d-spacings resulting from different draw rates or annealing temperatures



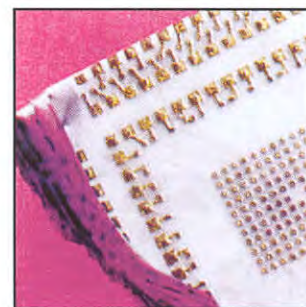
Texture

Measures scattering from amorphous through polycrystalline to 3-D single-crystalline with a powerful scripting feature



Composites

Versatile analysis of composite bondings with use of the system as an X-ray probe





Produced by
CCLRC
Daresbury Laboratory
for CCP13

Useful World Wide Web addresses (URL)

CCP13 Home Page
NCD Home Page
SRS Home Page

<http://www.dl.ac.uk/SRS/CCP13> ■
<http://www.dl.ac.uk/SRS/NCD>
<http://www.dl.ac.uk/SRS>